Spatio-temporal patterns of energy demand in New York City and implications for cogeneration

Draft Working Paper
January 3, 2010

Lily Parshall*, Hildigunnur Jónsdóttir, Stephen A. Hammer, and Vijay Modi

Abstract

This paper develops a spatially explicit model of energy demand in New York City. Load profiles are simulated for each individual New York City tax lot, with load disaggregated by end use, season, and time of day and all information linked to a GIS database. The model is then used to analyze the technical potential for distributed cogeneration. Potential reductions in primary energy demand and CO_2 emissions are estimated assuming that cogeneration is implemented in all technically feasible locations, where locations might include individual tax lots, groups of co-located tax lots, or blocks, depending on the scenario. We find that distributed cogeneration with small (~1 MW) gas turbines could add up to 709 MW of capacity across the five boroughs, reducing building-sector primary energy demand by 2.4% and CO_2 emissions by 7.9%, citywide. A district energy solution with larger generators may be able to deliver up to a 72.2% reduction in CO_2 emissions associated with buildings. Residential neighborhoods with multi-family buildings may be good sites for supply nodes because they tend to have thermal energy load that is several times larger than electric load. Overall, we show how a new approach to local energy planning, in which supply nodes emerge from the fabric of demand, can contribute to alternative energy development in cities.

*Corresponding author contact information:
llp15@columbia.edu
646-338-3599

1 Introduction

In centralized energy systems, buildings are demand nodes; in distributed generation (DG) systems, buildings can also be supply nodes. To understand whether DG can play a larger role in urban energy systems and what impacts DG might have on system design and efficiency, models that can match building load profiles with distributed supply options are needed. Such models can be used to scan a city or neighborhood to determine opportunities for DG, whether DG can increase energy efficiency and reduce greenhouse gas (GHG) emissions, what types of generators are suitable, and what unique urban factors influence the viability of DG.

In this paper, we focus on cogeneration (combined heat and power, or CHP), a DG technology that can dramatically reduce primary energy demand by recovering waste heat that is normally lost during electricity production, and using this energy to supply buildings with hot water, space heating, and/or space cooling. Cogeneration systems with the capacity to supply cooling, typically through an absorption chiller, are sometimes referred to as combined cooling, heating, and power (CCHP) or trigeneration systems.

Cogeneration is a commercially mature technology that can supply district energy systems or, at smaller scales, be integrated into individual buildings and cover all major building loads. Advantages of distributed cogeneration may include: ability to use waste heat, improving thermal efficiency of generation; reduction in transmission and distribution losses; ability to optimize local systems to match local demand profile; reduction in GHG emissions if cogeneration is less carbon-intensive than the existing fuel mix; and long-term cost savings. Disadvantages of cogeneration may include: high capital cost; local impacts including noise and/or air pollution; complexities and costs of interconnecting with the main distribution grid; and reliability and performance of generators and distribution networks.

This paper offers a spatially explicit analysis of the technical potential for cogeneration along with estimated energy and GHG emissions reduction benefits. Treatment of economic costs and market potential, as well as consideration of localized environmental benefits and costs such as changes in low-level air pollution and/or noise, is left for further research.

From the perspective of technical potential, densely populated, energy-intensive cities with temperate climates and mixed land use are good candidates for cogeneration because of their high density of demand for electric and thermal energy throughout the day and in multiple seasons. Cogeneration offers the largest GHG emissions reduction benefits in cities that rely on fossil fuels for the majority of their electricity and heat.

Urban areas consume two thirds of the world's energy, and at least 68% of urban consumption is associated with electricity and heat in buildings and industries (IEA, 2008).[1] Thus, it would be useful to have new energy planning tools to analyze supply and demand at the building scale and situate buildings within the overall context of urban blocks and neighborhoods. Our model takes the view that a city consists of interconnected energy conversion nodes and that municipal planners and policymakers can reshape urban energy systems by focusing on appropriate energy strategies at each viable node – whether it be an individual building, a cluster of complementary energy users, or a neighborhood (Andrews, 2008). Although we focus on cogeneration, the model could be extended to explore how the efficiency of urban energy systems might be improved through the integration of other alternative energy sources, local energy storage, building energy efficiency, and demand-side management.

[1] IEA (2008) estimated that cities account for 67% of primary energy demand. Of this, 32% is oil, which is used for transport, heating, and electricity production. The rest is consumption of fuels that are used primarily for electricity and heat. Therefore, we estimate that at least 68% of energy consumption in cities is associated with electricity and heat production.

In the model, we characterize several key aspects of building loads, including average electric and thermal loads, seasonal and diurnal variation in demand for each major end-use, and spatial location with respect to other supply and demand nodes. We characterize each building's energy demand based on its function(s), joining this information to a geodatabase that allows us to map urban energy demand on a tax lot-by-tax lot basis. In our cogeneration scenarios, we look for cases where individual buildings, or clusters of buildings, have a demand profile befitting a cogeneration supply node. Clusters of buildings represent potential micro-grid opportunities, with micro-grids typically defined as independent power distribution networks linking multiple generators and co-located customers, with a single point of interconnection to the main electricity grid (Abu-Sharkh et al., 2006; King, 2006).

New York City offers an ideal case study both because it has the right demand attributes and because the city government has specific goals concerning clean energy development and GHG emissions reductions. In 2007, New York launched PlaNYC, outlining the Mayor's vision for an environmentally and economically sustainable city. Cogeneration relates to two of the goals: 800 MW of additional clean, distributed generation and a 30% reduction in GHG emissions by 2030 (City of New York, 2007a). Utilizing our model, we show that technical potential for cogeneration is present in all five boroughs and may exceed 800 MW, the number of potential cogeneration supply nodes can be increased by clustering buildings, and the carbon footprint of the city's energy supply system could be reduced dramatically through the integration of distributed cogeneration.

2 Existing models and assessment tools

Most models of cogeneration feasibility begin by characterizing energy demand. There are many available general-purpose building simulation tools, such as eQUEST and other DOE-2 models;

20 of the best tools are reviewed in Crawley et al. (2005). Oak Ridge National Lab (ORNL) has developed a cogeneration-oriented building simulation tool called BCHP (ORNL, 2009). These tools are useful when a complete hourly load profile for each individual building is needed, but may produce more data than is needed for an energy planning exercise.

A few studies have linked simulated load curves with tax-lot data using a geographic information system (GIS). Examples include Dhakal et al. (2002) and Heiple and Sailor (2008), which model Tokyo and Houston, Texas respectively. In both cases, building simulation software is used to model prototypical buildings, with output attached to geographic data according to building category and size. The objective of these studies is to estimate hourly heat discharges into the urban environment to improve atmospheric models of urban climate and heat island mitigation. A third example is Yamaguchi (2007), which undertakes the same type of modeling to evaluate the impacts of various urban energy management strategies in Osaka; although the focus is on district-level strategies, conceptually, the demand side of the model is similar to our approach.

The planning philosophy guiding Yamaguchi (2007) is best described as community energy management (CEM), which analyzes the benefits of a particular energy strategy from the perspective of a local community (Jaccard et al., 1997). Similar studies include Sadownik and Jaccard (2001) and Chen et al. (2008). The latter analyzes a scenario in which individual building-scale generators are linked into a micro-grid serving a commercial district in Tokyo. In contrast to CEM, we allow individual buildings, or clusters of buildings, to emerge from our model, while CEM first designates neighborhood boundaries and then designs an energy management strategy. CEM asks “What benefits can cogeneration offer here?” We ask “Where might cogeneration offer the greatest benefits?”

Although a few DG studies employ spatial models, more common are energy-economic optimization models and other tools intended to maximize the value of a project through optimization of capacity, configuration and/or operating schedule. Many of these models are proprietary tools used for business development. There are only a few models that have been developed for the research community, most notably ORNL (2006). Both Gulli (2006) and Gustaffson and Roonqvist (2008) are recent examples of economic optimization applied to DG analysis. Gulli (2006) analyzes the value of cogeneration in Milan and Palermo, and Gustaffson and Roonqvist (2008) discuss alternative methods of heating residential buildings in Sweden.

The majority of cogeneration and micro-grid studies analyze Asian and European cities; King (2006) is one of the few models tailored to the United States. King (2006) determines the least-cost generation mix and operational schedule from the customer perspective, with each micro-grid modeled as a cluster of buildings with a particular customer mix and total load size. He finds that micro-grid value is most sensitive to the coincidence between heat and electric demand, followed by electric load factor and climate zone, and finally the magnitude of average demand. Load factor has only a moderate impact on micro-grid value because customers with a high load factor face large costs in both the base case and micro-grid scenarios; climate zone has only a weak influence on value because, although colder climates have larger demand for waste heat, seasonal variation reduces the efficiency of resource use (King, 2006).

Most research identifies the energy demand profile, and particularly the adequacy of thermal demand, as a key factor for the viability of cogeneration projects, but a wide range of technical, financial, regulatory, and market factors affect the feasibility of integrating small cogeneration plants into the urban energy system. CEMTPP (2007) provides a detailed summary of these factors in New York City, NYSERDA (2002) summarizes key issues affecting cogeneration market potential in New York State, and King (2006) discusses general regulatory issues in the United States. Interconnection with the main electricity grid is a particularly complex, and site-specific, concern treated at length in CEMTPP (2007).[2] Krause et al. (1994) compares the benefits and costs of centralized electricity systems and cogeneration. The analysis considers environmental externalities such as emissions of low-level air pollutants, as well as economic and policy uncertainties, offering a more complete evaluation of cogeneration potential than most other studies.[3] Availability and adequacy of gas supply is another major concern. These issues are beyond the scope of our analysis, but could be addressed as part of further research.

3 Background on New York City energy system

Many aspects of New York's energy system affect the potential for distributed cogeneration; we discuss only those factors that relate to supply and distribution of electricity and heat. New York is characterized by high density of demand for electricity and heat, a mix of fossil and renewable fuel sources, transmission constraints that require in-city electricity generation, one of the largest district heating systems in the world, and the small, but growing presence of small-scale (<10 MW) cogeneration.

[2] New York City's electricity distribution grid is owned and operated by Con Edison, a private company that enjoys a regulated monopoly on electricity transmission and distribution within the overall context of a deregulated electricity market. CEMTPP (2007) identifies a variety of challenges for distributed cogeneration supply, including operational compatibility with the grid, capacity limits, fault current, and standby tariffs.

[3] Krause et al. (1994) evaluates cogeneration in the Western European context as part of a larger study analyzing the CO_2 emissions reduction benefits and costs a range of electricity supply options. Three different perspectives on cost are offered: impact on electricity cost only, system-wide costs from a utility perspective, and system-wide costs including environmental externalities. The principal environmental externality, other than emissions of CO_2, is emissions of low-level air pollutants, including NO_x and SO_2. Localized environmental externalities depend on the specific technology and fuel source. In gas-fired cogeneration, low-level pollutant emissions are not necessarily larger than emissions from the stand-alone boilers that such systems replace. Appendix A.10.7 in Krause et al. (1994) includes a method for valuing the impact of cogeneration systems on low-level pollutants.

New York City's peak electricity demand is close to 11,500 MW (NYISO, 2008)[4], with about 50% of electricity produced at dedicated natural gas plants, 23% at oil/gas switching plants, 12% from nuclear, 6% from coal, 8% from hydro, and less than 2% from other renewables (City of New York, 2007b). Since the city is a load pocket, meaning that there is not enough transmission capacity to meet all demand with imports, state rules require there to be generation capacity located within the city that is capable of satisfying at least 80% of the city's summer peak demand, making distributed cogeneration an attractive option.[5] In 2005, about 57% of New York City's electricity was generated at in-city plants, which are combined cycle gas turbines (CCGT), combined cycle cogeneration, or oil/gas switching plants (City of New York, 2007b). Since most of New York City's electricity is generated at gas plants with high thermal efficiency (e.g. 50% for a CCGT compared to 30% for the typical coal plant), more than 20% of supply is non-fossil, and transmission losses are relatively small (~5%), the GHG emissions reduction benefits of small-scale cogeneration are less than in cities with a more carbon-intensive fuel supply. On the other hand, the severity of the transmission constraint adds to the appeal of in-city cogeneration.

Most of the city's large (>10 MW) cogeneration capacity supplies the district steam system, which serves 1,800 customers at 100,000 establishments between the Battery (southern tip) and 96th Street in Manhattan (Con Edison, 2009).[6] Total annual steam production in 2005 was 12,500 GWh. Despite the size of the steam system, it supplies just 11% of heat demand;

[4] In NYISO Control Zone J, which encompasses the five boroughs of New York City plus Westchester County, the highest peak demand on record is 11,347 MW. This peak was attained on August 2, 2006 at 4 PM. Note that prior to February 2005, New York City and Long Island were part of a combined control zone, with peak demand exceeding 15,000 MW.

[5] The installed local capacity totaled 8,800 MW in 2000, and transmission capacity allows for up to 5,000 MW of imported power (City of New York, 2004). Plants located within the city boundaries, or in nearby places linked to the city through dedicated lines, are included in the 80%.

[6] The district steam system, which is owned and operated by Con Edison steam, includes 105 miles of steam pipes in Manhattan. Commercial establishments account for about 64% of steam customers (Con Edison, 2009).

most heat demand is met with stand-alone boilers burning natural gas (62%) or fuel oil (27%) (City of New York, 2007b).[7] Producing heat in boilers is thermally efficient – typically less than 15% of the energy is lost during conversion – but the carbon intensity of fuel oil is about 35% higher than natural gas (Gurney et al., 2008).

Federally regulated cogeneration capacity in New York City is about 1100 MW, with the two steam-system plants accounting for about half of this (US EPA, 2002). Approximately 13% of New York City's electricity was cogenerated in 2000, with about 28% of this generated by the district steam system and the remainder generated at non-utility plants (US EPA, 2002).[8] As of 2007, there were an estimated 135 small (<10 MW) cogeneration plants with an aggregate capacity of 118 MW (CEMTPP, 2007). A variety of prime movers are used. Most older generators have reciprocating engines burning diesel fuels, and newer generators tend to employ gas-fired reciprocating engines or turbines (CEMTPP, 2007).[9] Most of these systems generate a portion of their electricity and purchase the rest from the grid. High real estate values make it prohibitively expensive to devote building floor space to plants large enough to completely cover load (CEMTPP, 2007).

Currently, cogeneration supply is below its potential in New York City, and additional cogeneration could help address projected demand shortfalls, transmission constraints, and emissions reduction goals (City of New York, 2004; City of New York, 2007a; CEMTPP, 2007). Based on a survey of building types and load sizes, NYSERDA (2002) identified 3200 MW of

---

[7] The share of heating demand supplied by steam has been declining, and the share supplied by natural gas has been rising (City of New York, 2007b), partly due to the high price of steam relative to natural gas. Within the city, natural gas is supplied to buildings via a series of pipelines linked to the national natural gas distribution system as there are no liquefied natural gas unloading terminals in the New York area.

[8] This is an estimate derived from data in US EPA (2002) and City of New York (2007b).

[9] The shift toward natural gas is related to technological breakthroughs such as the commercialization of gas-fired microturbines, interest in burning less carbon-intensive fuels, and dropping natural gas prices.

additional cogeneration potential in New York City.[10] Half of this is in hotels, hospitals, educational buildings, restaurants, and commercial laundries, which have been identified as appropriate on the basis of their relatively high annual heat-to-electric demand ratios (NYSERDA, 2002).

4 Urban energy planning model

Our model identifies possible sites where building demand nodes can become cogeneration supply nodes. We combine simulated building load curves with spatial data on building function and size and then identify cases where the demand profile matches a cogeneration technology scenario. Our model was constructed with the energy planner in mind, so we scan an entire city for cogeneration opportunities and then compute potential reductions in fossil-related primary energy demand and CO_2 emissions based on incorporating these new supply nodes into the urban energy system. There are four main steps in the model: [1] construction of building load profiles, [2] characterization of technology scenarios, [3] matching of demand profiles with cogeneration supply, and [4] quantification of cogeneration benefits.[11]

4.1 Building load profiles

We create building load profiles by estimating annual energy intensity (demand per m^2), disaggregated by end use, for different building functions. Then, we determine the portion of annual intensity that occurs in different seasons at different times of day. End use is divided into

---

[10] NYSERDA (2002) assessed cogeneration potential in each utility's service territory. Con Edison operates in the five boroughs of New York City plus Westchester County, with New York City responsible for 87% of demand within the service territory (CEMTPP, 2007).

[11] The model was built in Stata, a data analysis software package.

base electric (lighting, appliances, etc.), space cooling, hot water, and space heating.[12] Total energy load for each building at each point in time is computed by multiplying the intensity numbers for each building function by that function's area. Our approach captures key elements of annual demand variation without running building simulation software and allows us to model multi-function buildings.

4.1.1 Annual energy intensity for each building function

We define 15 different building functions. The functional categories reflect the US Department of Energy's (US DOE) building categories, with some modifications to reflect how building functions are defined in the New York City MapPLUTO (PLUTO) database developed by the Department of City Planning (NYC Planning) (US DOE, 2003; NYC Planning, 2008). PLUTO includes information on gross building area for each of several different building functions for each tax lot within the five boroughs. There are approximately 1 million buildings on 855,099 lots in New York City; limitations of PLUTO meant we were not able to distinguish between individual buildings on the same lot. We reclassified PLUTO to determine the building area within each of our 15 functional categories on each lot.[13]

Annual energy intensity for each building function was estimated using Huang et al. (1991), US DOE (2003), City of New York (2007a), and City of New York (2007b). We first used data from City of New York (2007b) to estimate total final consumption (delivered energy) in New York City buildings, which in 2005 was approximately 162,000 GWh, of which 47,000

[12] Space cooling covers ventilation as well as air conditioning. Demand for cooking, which might be met with electricity or natural gas was grouped with base electric since this category includes appliances. In practice, many buildings use natural gas for cooking. Buildings with cogeneration systems would either meet cooking demand through a direct natural gas connection or with electricity produced by the system; since demand is relatively small, we do not explicitly consider it in our model. Industrial buildings may use heat for industrial processes; we do not separate this from space heating.

[13] The reclassification process was based on building class codes and floor area categories contained in the PLUTO database.

GWh (29%) was electricity consumption.[14] The remainder was consumption of steam and major fuels, including natural gas, and distillate and residual fuel oil. We adjusted these data to obtain estimated per-square-meter building loads, with building load defined as the energy input required assuming that all building equipment runs at 100% efficiency. In the model, building load intensities are the metric used to represent energy intensity for each end use. To convert from the electric intensity of space cooling to building load intensity, we multiplied space cooling intensities by an assumed air conditioning coefficient of performance (COP) for each building function. An air conditioner typically produces several units of cooling for each unit of electricity consumed, so electric intensity for space cooling may underestimate energy required for cooling if absorption chilling replaces electric chilling. We also adjusted heating and hot water intensities to account for boiler efficiency, reducing these numbers by 15% to convert from fuel intensities to building load intensities.

After these adjustments, we estimated city wide building load to be 166,900 GWh, of which 30% was base electric (lighting, appliances), 18% space cooling, 15% hot water, and 37% space heating. We then set a constraint on total simulated citywide energy demand such that:

$$\sum_{i=1}^{15}\sum_{j=1}^{4} d_{i,j} * B_i = T_{sn} \qquad [1]$$

where $d_{i,j}$ is the load intensity for each end use j and building function i, B_i is total building area for each function, and T_l is total building load.

[14] City of New York (2007b) estimated total electricity and fuel consumption by gathering data from utility and fuel oil suppliers operating in New York City. The estimates supplied here exclude fuel consumption for transportation. 2005 estimates were not adjusted to account for inter-annual weather variation, which affects space heating and cooling demand.

When combined with PLUTO data on building function, City of New York (2007a and 2007b) contained enough data to estimate annual load intensity for residential and industrial categories, but not commercial and institutional intensities. Huang et al. (1991) simulated energy demand in 481 prototypical buildings, where each building had a specific function (e.g., hospital, office), was located in a specific city (e.g., New York), and had a particular stock and equipment vintage (e.g., pre-1980 construction with old equipment, pre-1980 with new equipment, post-1980 with new equipment). For commercial building functions covered by Huang et al. (1991), our intensity estimates were based on an average of old stock/old equipment and old stock/new equipment, since 89% of New York's building stock predates 1980 (City of New York, 2008).[15] For the remaining commercial building functions, we used US DOE (2003). In this case, we applied nation-wide averages to New York City, an approach consistent with NYSERDA (2002).

In New York City, HDD and CDD are 11% higher and 16% lower, respectively, compared with the United States (NREL, 2008). Therefore, this approach should not have introduced a large amount of error. Nonetheless, our initial estimates of commercial and institutional demand were 62% lower than expected based on City of New York (2007a and 2007b). Building energy demand is affected by many other factors including building age, envelope and design; heating and cooling equipment; type of tenant(s) and tariff schedule(s); occupancy and operating schedule(s); and tenant behavior. Commercial and institutional buildings in New York tend to be older than the U.S. average, and a large fraction of office floor area is occupied by energy-intensive industries such as financial services. Since we were confident in the end-use breakdowns from Huang et al. (1991) and US DOE (2003), but not in the magnitude of the

[15] We excluded new stock/new equipment because such a small percentage of New York's building stock was constructed within the past 30 years. Even after this exclusion, our estimated energy intensities were lower than expected based on comparisons with actual New York City data.

intensities, we scaled up the initial intensities to satisfy Equation [1].[16] Table 1 summarizes the percentage breakdown across building functions in New York City, end use intensities for each building function, and assumed COPs for electric chilling in the base case.

Total energy demand, measured as building load, for each New York City tax lot (k) was calculated by multiplying end use intensities by floor areas:

$$D_{k,j} = \sum_{i=1}^{15} d_j * b_i \quad for\ j=1,\ldots,4;\ k=1,\ldots,K \qquad [2]$$

where $D_{k,j}$ is total energy demand for end use j, b_i is the fraction of building floor area with function i and K is 855,099.

4.1.2 Seasonal and diurnal variation

We divided annual energy demand for each end use into 12 months and then into 6 diurnal usage levels within each month:

$$D_{k,j,m,t} = u_{k,t} * q_m * D_{k,j} \quad for\ j=1,\ldots,4;\ k=1,\ldots,K;\ m=1,\ldots,12;\ t=1,\ldots,6 \qquad [3]$$

where $D_{k,j,m,t}$ is annual demand for end use j in tax lot k during month m and usage period t, q_m is the percent of total annual demand that occurs in month m, and $u_{k,t}$ is the percent of total monthly demand that occurs in usage period t for building k. This produces 288 demand values for each building: 72 demand tranches x 4 end uses. Note that the distribution across usage levels depends on building function:

$$u_{k,t} = \sum_{i=1}^{15} u_{i,t} * b_i \quad for\ k=1,\ldots.,K;\ t=1,\ldots,6 \qquad [4]$$

[16] Commercial intensities were multiplied by 1.70, and institutional intensities were multiplied by 1.42. After applying these factors, total commercial and institutional demand was equal to citywide demand for each of these categories in City of New York (2007b).

Table 1. Building functions and annual end use intensities.

Building function	Percent of total floor area [a]						Annual energy intensity (kWh/m^2) [b]					Ratio (base electric: thermal	COP (electric chiller) [c]
	Manhattan	Bronx	Brooklyn	Queens	Staten Island	Total	Base electric	Thermal: Space cooling	Thermal: Hot water	Thermal: Space heating	Total		
1 & 2 family	0.3%	2.1%	7.0%	8.7%	3.8%	21.9%	34	13	40	117	205	4.93	2.5
3 & 4 family	0.2%	0.8%	3.0%	1.6%	0.1%	5.7%	34	13	40	117	205	4.93	2.5
Walk-up	2.9%	2.1%	3.2%	1.7%	0.1%	10.0%	39	17	82	82	220	4.63	2.5
Multi-family	12.4%	4.8%	6.2%	4.7%	0.5%	28.7%	39	17	82	82	220	4.63	2.5
Residential	**15.8%**	**9.9%**	**19.4%**	**16.6%**	**4.5%**	**66.2%**	-	-	-	-	-	-	-
Education	1.0%	0.8%	1.2%	0.9%	0.2%	4.1%	112	21	23	175	331	1.96	3
Health	0.8%	0.3%	0.4%	0.3%	0.1%	1.8%	357	209	176	374	1,116	2.13	3
Lodging	0.9%	0.1%	0.1%	0.1%	0.0%	1.1%	167	109	47	422	746	3.47	3
Public Assembly	0.4%	0.0%	0.1%	0.1%	0.6%	1.2%	142	129	4	189	465	2.27	3
Public Order	0.1%	0.0%	0.0%	0.0%	0.0%	0.2%	258	90	267	105	720	1.79	3
Religious	0.5%	0.1%	0.4%	0.3%	0.0%	1.4%	58	39	3	99	199	2.46	3
Institutional	**3.7%**	**1.4%**	**2.1%**	**1.6%**	**0.9%**	**9.8%**	-	-	-	-	-	-	-
Office	7.8%	0.3%	0.8%	0.7%	0.1%	9.7%	285	242	7	205	739	1.59	3.5
Store	2.2%	0.5%	1.2%	1.0%	0.2%	5.1%	259	173	4	89	525	1.03	3.5
Warehouse	1.2%	0.4%	1.0%	0.7%	0.1%	3.3%	129	26	3	88	246	0.90	3.5
Other Commercial	1.2%	0.3%	1.3%	1.0%	0.1%	3.9%	364	194	10	362	931	1.56	3.5
Commercial	**12.4%**	**1.5%**	**4.2%**	**3.4%**	**0.5%**	**22.0%**	-	-	-	-	-	-	-
Industrial	**0.1%**	**0.3%**	**0.9%**	**0.7%**	**0.1%**	**2.0%**	294	130	135	167	726	1.47	3
Total	**32.0%**	**13.0%**	**26.7%**	**22.3%**	**6.0%**	**100.0%**	-	-	-	-	-	-	-

(a) Total floor area in New York City is approximately 476 million m^2 (NYC Planning, 2008). (b) Annual energy intensities are building load intensities. (c) Assumed coefficient of performance (COP) for electric chilling. Annual energy intensity for space cooling divided by the COP gives an estimate of electric demand for cooling in the base scenario.

We also computed the average hourly demands ($\overline{D}_{k,j,m,t}$), which are important to estimate needed generation capacity as well as load factors:

$$\overline{D}_{k,j,m,t} = \frac{D_{k,j,m,t}}{h_{m,t}} \quad \textit{for } j=1,\ldots,4;\ k=1,\ldots,K;\ m=1,\ldots,12;\ t=1,\ldots,6 \qquad [5]$$

Note that the number of hours in each demand tranch $h_{m,t}$ varies depending on the length of the month.

Monthly divisions were based heating degree-days (HDD) for space heating, cooling degree-days (CDD) for space cooling, and the number of hours in each month for base electric and hot water.[17] The parameters used to capture seasonal demand variation are in Table 2. HDD and CDD were derived from a typical meteorological year (TMY) in New York City, which has 4957 heating degree days, most of which occur between November and April, and 1112 cooling degree days, most of which occur between June and September (NREL, 2008).

Table 2. Estimated percentage of annual demand that occurs in each month for each end use.

Month	Base electric (%)	Space cooling (%)	Hot water (%)	Space Heating (%)
January	8.5	0.0	8.5	22.6
February	7.7	0.0	7.7	17.1
March	8.5	0.0	8.5	13.3
April	8.2	1.7	8.2	8.1
May	8.5	8.9	8.5	3.2
June	8.2	19.0	8.2	0.1
July	8.5	33.5	8.5	0.0
August	8.5	24.6	8.5	0.1
September	8.2	11.7	8.2	0.6
October	8.5	0.6	8.5	6.1
November	8.2	0.0	8.2	10.3
December	8.5	0.0	8.5	18.5

[17] CDD = T_{mean}-18.3˚C (65˚F) if T_{mean}>18.3˚C, where T_{mean} is the mean daily temperature. HDD=18.3- T_{mean} if T_{mean}<18.3˚C. Total HDD/CDD for each month is the sum of daily HDD/CDD.

The 6 diurnal usage levels were based on building occupancy schedules for different building functions (Huang et al., 1991). The divisions were: (1) weekday morning, 6-8 AM, (2) workday, 8 AM-5PM, (3) weekday evening, 5-10 PM, (4) night, 10 PM-6 AM, (5) weekend morning, 6 AM-12 PM, and (6) weekend afternoon, 12-10 PM. We assumed that building occupancy affects 25% of demand. This percentage was chosen because it resulted in monthly peak demand of approximately twice monthly average demand, a relationship reflected in utility bill data from a sample of New York City buildings. The parameters used to capture diurnal demand variation are in the appendix, in Table A1.

Reducing diurnal variation from 8760 hours to 72 usage levels for each end use reduces the number of calculations required to analyze building load by 99%, but may miss some important aspects of diurnal variation. For example, Heiple and Sailor (2008) show that such an approach does not capture the morning warm-up and subsequent attenuation of demand for space heating in commercial buildings during the winter.

In commercial buildings, space heating demand is lower in the middle of the day than in the morning because people and equipment give off heat, and because the ambient air temperature is generally higher. In the summer, demand for space cooling rises in the middle of the day since these factors must be counteracted. Also, the model assumes an 8 AM-5 PM workday, but in reality, many businesses in New York City have a longer workday.

In residential buildings, demand for space heating and cooling tends to be lower during working hours; the former due to the diurnal weather profile and the latter due to lower occupancy. Our model does capture this feature of residential buildings, but may underestimate the magnitude of attenuation during the workday. Further research could improve how diurnal variation is characterized in the model.

4.1.3 Comparing simulated building load curves with utility bill data

We compared our simulated building load curves with monthly utility bill data collected from a sample of New York City buildings. Utility bill data include information on electricity and fuel consumption; we estimated base electric consumption by assuming that consumption in non-cooling months (November-March) is base electric (lighting, appliances, etc.) and that any additional consumption is space cooling. Utility bill data from specific buildings were compared to the simulated base case, which assumes electric chilling and converts building load estimates to final consumption of electricity and fuel for consistency with utility bill data. Figure 1 shows two examples of comparisons between our model and utility bill data.[18] These comparisons reveal that our monthly load shapes reflect actual seasonal variation in demand in New York City, but that the magnitude of individual building loads, and particularly thermal loads, are likely to be over- and/or under-estimated. It makes sense that we overestimate loads in some buildings and underestimate them in other buildings since the end-use intensities underlying our model represent citywide averages. We also expect errors for individual buildings since we use 15 functional categories to represent 1 million unique buildings. Nonetheless, our model approximates load shapes for individual end uses with reasonable accuracy, allowing us to identify potential opportunities for cogeneration. Estimates of cogeneration capacity and emissions reductions may be less accurate since they are affected by the magnitude of simulated load size. The use of actual data, supplied by local utilities, would improve the validity of the model.

[18] Due to confidentiality agreements, we are not able to disclose the exact addresses associated with the utility bill data.

a)

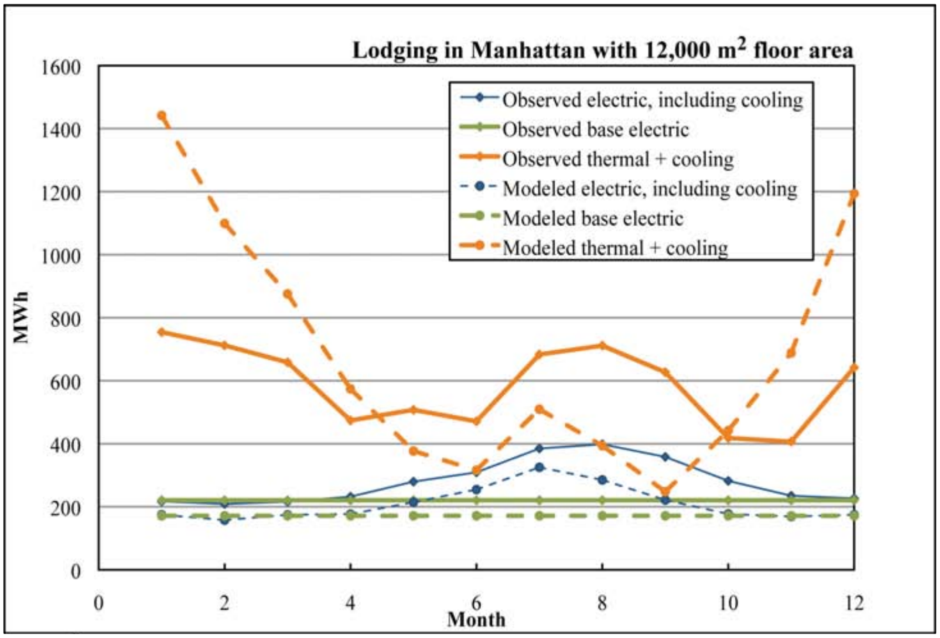

b)

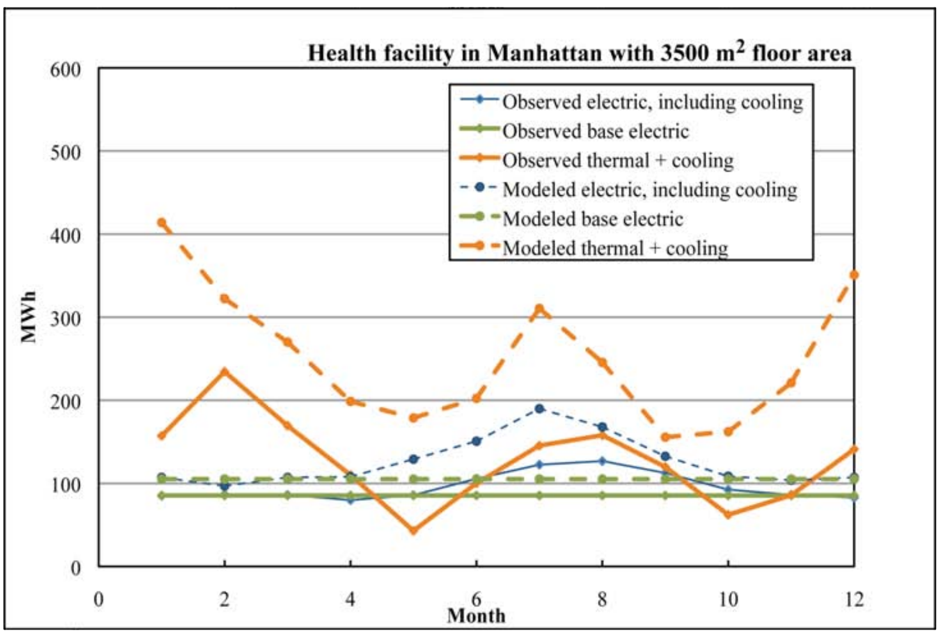

Figure 1. Comparison between simulated base case and utility bill data. a) Lodging. b) Health.

4.2 Technology scenarios

The technology scenarios consist of gas-fired prime movers, with absorption chillers to supply cooling. We assume that each supply node must have at least one large anchor building, and that supply nodes must be continuous thermal sinks. In other words, there must be enough thermal demand within the node to run the generator at all times and to use all the waste heat that is produced. We assume that cogeneration systems will be thermal load following, so the amount of electricity produced depends on thermal demand.[19] These criteria allow us to identify cases where cogeneration is most likely to be viable and where the potential system-wide emissions reduction benefits are largest. Cases where cogeneration might be a good peak shaving or backup generation strategy, but cannot supply base load, are not included. This is a key difference between our evaluation of cogeneration potential and studies of building-scale economic feasibility that often analyze situations where cogeneration may not be in operation at all times. Clusters of buildings are identified as nodes only in cases where a potential anchor building is not a continuous thermal sink unless joined with one or more adjacent buildings. We also identify city blocks that are continuous thermal sinks. In all cases, we assume that electricity produced to meet thermal demand, but not used on site, can be sold into the grid.[20] The feasibility and economics of net metering, which would be required as part of this scenario, are beyond the scope of the analysis.

---

[19] In cogeneration systems that are thermal load following, covering thermal load is the priority. Depending on the thermal-to-electric ratio of energy demand, and of the cogeneration system, the amount of cogenerated electricity may fall short of or exceed on-site demand. A connection to the main electricity grid typically functions as a source and/or sink for cogenerated electricity. In systems that are electric load following, covering electric load is the priority. At times when the system does not produce enough heat to cover thermal load, on-site boilers are typically used to cover the shortfall. If the system produces more heat than is needed, the excess heat is typically vented to the atmosphere.

[20] Continuous thermal sinks will constantly produce extra electricity that is sold to the grid, but will not need to purchase electricity from the grid or run a boiler.

4.2.1 Cogeneration technology

Cogeneration systems include a fuel source, a prime mover with a heat recovery system, an absorption chiller if cooling demand is to be covered, grid lines for electricity distribution, hot water or steam pipes for heat distribution, and chilled water pipes for distributing cooling. We do not include grid lines or pipelines in our model because we do not consider distribution constraints. We assume that all systems have absorption chillers and that all cooling demand will be met with an absorption chiller. Our model analyzes technical feasibility of cogeneration, so we do not consider the economics of different systems.

Prime movers include steam turbines, internal combustion (IC) engines, gas turbines, microturbines, and fuel cells. Each prime mover has specific technical specifications that affect its suitability for particular applications; these include fuel source(s) and pressure, size ranges, footprint (space required per kW of capacity), amount of useable heat that is produced per unit of electricity production, temperature and potential uses of recovered heat, black start time (amount of time between switching on a generator and producing electricity), running hours between scheduled maintenance, part load performance (reduction in efficiency when generator is operated below rated capacity), commercial status, capital cost per kW of capacity, cost per kWh of energy produced, noise, emissions of local air pollutants (NOx, CO, SO_2, PM, VOCs), and emissions of GHGs (principally CO_2) (NYSERDA, 2002; CEMTPP, 2007; US EPA, 2009).

In our technology scenarios, we assume gas turbines are the prime mover because they are a commercial technology available in a wide range of sizes, can run continuously for several years without requiring off-line maintenance, can directly supply high-quality heat, and have low operating costs, all of which make them suitable as the primary source of electricity and heat for distributed demand nodes.[21] We consider standard, single-cycle gas turbines, rather than combined cycle gas turbines because although cogeneration with CCGT can achieve efficiencies of up to 85%, more than 15% higher than combustion turbines, they are typically applied at the utility scale in large sizes (>100 MW) and therefore are better suited to district energy systems serving neighborhoods or cities. Microturbines, which are available in sizes as small as 30 kW, are not considered because they typically cover a small portion of total building load (e.g. hot water plus a fraction of electricity demand). But multi-unit microturbine arrays, which are gaining in popularity, may be a suitable choice for small nodes (< 1 MW) and could be modeled as part of further research.

We compare small gas turbines, which have a lower heat-to-electricity ratio, with medium gas turbines, which have a higher thermal efficiency. We characterize a small gas turbine based on the typical performance of a 1 MW turbine; our medium gas turbine is characterized as a 10 MW turbine. In the small-turbine scenarios, we assume that regardless of node size, one or more generators with the heat-to-electric ratio typical of a 1 MW turbine would supply the node. In the medium-turbine building scenario, we assume that nodes must have a minimum size of 10 MW. In the block scenarios, we assume that medium turbines would serve one or more co-located blocks. Parameters characterizing prime movers, including heat-to-electric ratios, can be found in Table 3.

[21] IC engines can reach higher thermal efficiencies and have better part-load performance than gas turbines. Although IC engines are common in cogeneration applications, they are suitable only in cases where total load size is less than 5 MW. Also, small IC engines can supply hot water, but not space heating. Therefore, they are not modeled. Fuel cells are not considered because they are not yet available on a commercial scale.

Table 3. Model parameters and data sources.

Parameter	Description	Eqn(s)	Scenario(s)	Value [a]	Data source
c_{grid}	Thermal efficiency of grid electricity	8,13	base	0.5	calculated [b]
c_{loss}	Transmission and distribution losses	8,13	base	0.0527	City of New York (2008)
c_{gcog}	Percentage of grid electricity cogenerated in base case	8,13	base	0.125	US EPA (2002)
c_{boil}	Thermal efficiency of boiler in base case	8	base	0.85	City of New York (2008)
c_{abs}	COP of absorption chiller	6,9	1,2,3,4,5,6	0.7	New Buildings Institute (1998)
CO_2 emissions					
e_{grid}	CO_2 emissions per unit of grid electricity, including generation, transmission, and distribution losses	17,20	base	446 tons per GWh	City of New York (2008)
p_{natgas}	Percent heating demand met with natural gas in base case	16	base	0.61	City of New York (2007b)
p_{dist}	Percent heating demand met with distillate oil in base case	16	base	0.20	City of New York (2007b)
p_{resid}	Percent heating demand met with residual oil in base case	16	base	0.08	City of New York (2007b)
p_{steam}	Percent heating demand met with steam in base case	16	all	0.11	City of New York (2007b)
e_{natgas}	CO_2 emissions per unit of natural gas consumption	16,18	base	181 tons per GWh	Gurney et al. (2008)
e_{dist}	CO_2 emissions per unit of distillate oil consumption	16	base	250 tons per GWh	Gurney et al. (2008)
e_{resid}	CO_2 emissions per unit of residual oil consumption	16	base	269 tons per GWh	Gurney et al. (2008)
e_{steam}	CO_2 emissions per unit of steam consumption	16	base	191 tons per GWh	City of New York (2008)
e_{heat}	Weighted average CO_2 emissions per unit of heat consumption	16,17	base	203 tons per GWh	calculated
Small gas turbines (~1 MW, total thermal efficiency=0.674)					
c_{cog}	Thermal efficiency of cogenerated electricity	11	1,2	0.208	US EPA (2009)
c_{wh}	Available waste heat per unit of cogenerated electricity	6,9	1,2	2.25	US EPA (2009)
Medium gas turbines (~10 MW, total thermal efficiency=0.711)					
c_{cog}	Thermal efficiency of cogenerated electricity	11	3,4,5,6	0.290	US EPA (2009)
c_{wh}	Available waste heat per unit of cogenerated electricity	6,9	3,4,5,6	1.45	US EPA (2009)

(a) Parameter values are dimensionless unless otherwise noted. (b) Calculated based on prime mover information in City of New York (2007b) and thermal efficiencies from Thumann and Mehta (2008) and Energy Blueprint (2009).

Absorption chillers convert heat energy (in the form of hot water or steam) into cooling energy (in the form of chilled water), with a small amount of electricity required for compression and/or pumps, fans, and controls. There are several types of chillers including direct-, indirect-fired, and hybrid (gas/electric), and each of these can be single- or double-effect. Indirect-fired chillers that make use of waste heat, rather than a direct source of fuel, are typically used in cogeneration applications. Double-effect chillers have two condensers and generators to increase thermal efficiency. In our model, we assume single-effect chillers because, although less thermally efficient (COP of approximately 0.7) than double-effect chillers (COP of approximately 1.2), they are less expensive and generally sufficient when there is a readily available source of waste heat (New Buildings Institute, 1998).

From the standpoint of technical potential, the inclusion of an absorption chiller can help to balance electric and thermal loads in the summer in buildings that have a substantial thermal load (e.g., multi-family residential buildings that have high hot water intensity and central air conditioning). But absorption chillers are more expensive than electric chillers and can render project economics unfavorable, particularly for commercial buildings that have small thermal loads in the summer. The scenarios we consider in this paper, which include an absorption chiller and assume thermal load following, represent a few examples of the large number of possible cogeneration system configurations and operational modes. Depending on the specific building load profile, as well as tariff structure and other economic incentives, different configurations may make sense in different locations.

4.3 Identification of cogeneration nodes

Each node is seeded with an anchor building, with the footprint and/or size of the building varying depending on the scenario. In New York City, space is a premium commodity. Many buildings do not have the space, or do not want to give up space, to host a generator. The anchor-building concept is intended to restrict cogeneration nodes to locations most likely to have space to host a generator; removing this restriction would substantially increase the number of nodes identified.

In most of our scenarios, the anchor building must have a footprint of 2500 m^2.[22] Since the PLUTO data are organized by lot, not by individual building, this is the total estimated footprint (measured as the building area divided by the number of floors) for the lot. In practice, many of the lots identified as anchors contain multiple buildings; also in buildings that taper as they rise, the footprint is underestimated. In one scenario, we define the anchor as a development with at least 32,515 m^2 (350,000 ft^2) of gross floor area. New York City is considering a requirement that new developments of this size complete a cogeneration feasibility study; we evaluate the scale of opportunity for existing buildings above this size threshold.

When we search for possible cogeneration nodes, we do not mask buildings that currently have cogeneration, so we may over estimate new cogeneration potential by 100-200 MW.[23] We also do not mask buildings that are currently connected to the district steam system as this information is not publicly available. These buildings may have less space to install a generator and/or be less interested in replacing a steam connection with a cogeneration plant compared with buildings that already have a boiler room. We do, however, include a scenario where all buildings within the steam system zone are excluded from becoming cogeneration nodes.

In each scenario, we first identify buildings that meet the anchor criteria. Next, we define a technology scenario, which includes the relationship between electricity production and waste

[22] This is a somewhat arbitrary threshold based on discussions with local stakeholders. A high threshold is set to avoid overestimation of potential capacity.

[23] Masking individual buildings is a laborious process that requires identifying each building with cogeneration.

heat production. Then, we search for anchor buildings that are continuous thermal sinks such that, for tax lot (*k*):

$$Elcb_{k,m,t} * c_{wh} < heat_{k,m,t} + hotw_{k,m,t} + \frac{cool_{k,m,t}}{c_{abs}} \quad for\ m=1,\ldots,12;\ t=1,\ldots,6 \qquad [6]$$

where *Elcb* is base electric load, *heat* is space heating load, *hotw* is hot water load, *cool* is space cooling load, c_{wh} is the amount of waste heat produced per unit of electricity production, and c_{abs} is the COP of the absorption chiller. Base electric load does not include electricity demand for ancillary equipment, gas compression, or to run the absorption chiller, all of which would increase *elcb* during cogeneration.[24] The exclusion of these electric loads means that we may overestimate the number of continuous thermal sinks and/or the amount of electricity that is sold to the grid in our technology scenarios.[25]

In cases where an anchor building is not itself a continuous thermal sink, we look for opportunities to cluster buildings adjacent to the anchor. Clustering buildings with different functions can reduce diurnal variation in load, for example by grouping commercial buildings that have a daytime, weekday peak with residential buildings that have their largest energy demand in the evening and on weekends. The clustering algorithm has the following steps:

1) Define technology scenario, including anchor-building definition.
2) Search building data for anchor buildings.
3) Check each anchor building to determine whether it is a continuous thermal sink; if so, designate building as a cogeneration supply node.
4) If not, use a spatial algorithm to identify the anchor building's 9 nearest neighbors (NN).[26]

---

[24] Absorption chillers consume electricity to run the chiller, condenser water pumps, cooling tower, and hot water pumps; estimated total electricity consumption is 6-8% of the system size and about 20% of the electricity used to run an electric chiller of equal capacity (Jayamaha, 2006).

[25] Most of the continuous thermal sinks we identify have thermal load that is several times higher than base electric load, which is the case for multi-family buildings. Therefore, although we may overestimate the amount of electricity sold, and associated benefits, it is unlikely that this leads to many cases where supply nodes are misidentified.

[26] To define NNs, we use an algorithm available in Hawth's Tools in the ArcGIS software package.

5) Check to see whether anchor building plus the 1st NN is a continuous thermal sink; if so, designate the 2-building cluster a cogeneration supply node.
6) If not, check the 2nd NN, followed by up to 9 NN, stopping if a match is found.
7) If, after checking 9 possible 2-building clusters, no match is found, check 3-building cluster consisting of the anchor building plus the 1st NN plus the 2nd NN; if this cluster is a continuous thermal sink, designate the 3-building cluster a cogeneration supply node.
8) If not, check 4-building cluster consisting of anchor building plus 3 NNs, checking clusters of up to 10 buildings and stopping if a match is found.
9) The set of feasible cogeneration supply nodes consists of individual anchor buildings, 2-building clusters, and multi-building clusters that are continuous thermal sinks.[27]

We prefer smaller clusters, composed of buildings as close to the anchor as possible, because these clusters are likely to have lower electric and heat distribution costs, and because coordination challenges increase with the number of buildings within the supply node.

In some technology scenarios, we look for cogeneration supply nodes at the scale of city blocks. In these scenarios, we do not define an anchor building, and we do not implement a clustering algorithm. Block scenarios are intended to represent the upper bound of citywide distributed cogeneration potential.

Some of the nodes that we identify may be better candidates than others, depending on capacity requirements, electric and thermal load factors, the percentage of total electricity produced that can be used within the node, and the building function(s) represented within the node. Since all the nodes are continuous thermal sinks, thermal efficiency is equal to the rated value for the prime mover in the scenario (see Table 3). Although we keep track of a variety of secondary characteristics of each node in the model, we do not cull potential supply nodes on the basis of these characteristics.

[27] The current version of the clustering algorithm checks specific sets of nearest neighbors; as part of further research, an expanded algorithm that checks a much larger set of possible groupings could be developed.

4.4 Benefits of cogeneration supply nodes

We quantify the annual benefits of each cogeneration node in terms of reductions in fossil-based primary energy demand, CO_2 emissions, and cogeneration capacity. We define the *local* benefit of an individual node as the reduction in primary energy demand/CO_2 emissions within the node compared to the base scenario of supplying the node with grid electricity and heat produced by a boiler for one year. The *system* benefit of the set of cogeneration supply nodes is defined as the reduction in primary energy demand/CO_2 emissions in the city, after accounting for cogenerated electricity that is sold into the grid.

4.4.1 Primary energy demand

In the base scenario, we assume that space cooling load is met with an electric chiller. Therefore, before computing base primary energy demand, we first adjust cooling load to reflect the COP for air conditioning for each building function:

$$ecool_{k,m,t} = \sum_{i=1}^{15} cool_{k,m,t} * b_i * ecop_i \qquad [7]$$

where $ecool_{k,m,t}$ is the electric load for cooling for tax lot k in month m and usage period t, and $ecop_i$ is the typical COP for building function i (see Table 1). Then, for each node n, total base primary energy demand is computed as:

$$PE_{base,n} = \underbrace{(1 + c_{loss}) * (\frac{1}{c_{grid}}) * (1 - c_{gcog}) * \sum_{m=1}^{12}\sum_{t=1}^{6}(elcb_{n,m,t} + ecool_{n,m,t})}_{PE_{base,elec,n}} + \underbrace{(\frac{1}{c_{boil}}) * \sum_{m=1}^{12}\sum_{t=1}^{6}(hotw_{n,m,t} + heat_{n,m,t})}_{PE_{base,heat,n}}$$

[8]

where c_{loss} is transmission and distribution losses associated with grid electricity, c_{grid} is the overall thermal efficiency of grid electricity, c_{gcog} is the percentage of grid electricity that is currently cogenerated, and c_{boil} is the thermal efficiency of heat production. We avoid double-counting primary energy demand associated with existing cogeneration by adjusting $PE_{base,elec,n}$ downward. End-use loads *(elcb, ecool, hotw, heat*) for each node (n) are the sum of end-use loads for each tax lot (k) within the node. The values of all model parameters (e.g., c_{loss}, c_{grid}, c_{gcog}, c_{boil}), along with data sources, are shown in Table 3.

The amount of electricity generated at the supply node (cog_n) is determined by thermal demand:

$$cog_n = \sum_{m=1}^{12}\sum_{t=1}^{6}\left[\frac{1}{c_{wh}} * (\frac{cool_{n,m,t}}{c_{abs}} + hotw_{n,m,t} + heat_{n,m,t})\right] \quad [9]$$

The portion of this consumed within node n is $elcb_n$. Therefore, the portion sold to the grid is:

$$esold_n = cog_n - elcb_n \quad [10]$$

Because the node is a continuous thermal sink, electricity production is continuously greater than on-site demand. Therefore, $esold_n$ is always greater than 0.

Primary energy consumed for cogeneration within supply node n is:

$$PE_{cog,n} = \frac{1}{c_{cog}} * cog_n \quad [11]$$

where c_{cog} is the thermal efficiency of electricity generation at the cogeneration plant, assuming there are no transmission and distribution losses within the node. Therefore, the *local* change in primary energy is:

$$benefit_{PE,local,n} = PE_{cog,n} - PE_{base,n} \quad [12]$$

Note that negative values of $benefit_{PE,local}$ indicate a reduction in primary energy demand. In cases where $esold_n$ is large, $PE_{cog,n}$ may be larger than PE_{base} before accounting for grid electricity that is displaced by $esold_n$.

The *system* reduction in primary energy demand is the sum of the *local* benefits of all cogeneration supply nodes plus the benefits of electricity sold into the grid over a one-year period. Displaced primary energy demand associated with electricity sold by a cogeneration supply node n is:

$$PE_{displ,n} = (1 + c_{loss}) * (\frac{1}{c_{grid}}) * (1 - c_{gcog}) * esold_n \qquad [13]$$

Therefore, the *system* reduction in primary energy demand is:

$$benefit_{PE,system} = \sum_{n=1}^{N} (benefit_{PE,local,n} - PE_{displ,n}) \qquad [14]$$

Note that base primary energy demand, citywide is:

$$PE_{base,system} = \sum_{k=1}^{K} PE_{base,k} \qquad [15]$$

4.4.2 CO_2 Emissions

We focus on CO_2 emissions reductions, rather than total GHG emissions reductions because more than 99% of GHG emissions associated with electricity and heat production in New York City are CO_2 (City of New York, 2008). We first estimate CO_2 emissions associated with the base case of grid electricity and heat from a boiler. Our estimate of 446 tons per GWh for grid electricity was derived from City of New York (2008), with generation, transmission, and distribution losses accounted for. This is the value of e_{grid} in Equation [17]. To estimate emissions associated with heat production (e_{heat}), we computed a weighted average CO_2

coefficient based on the portion of heat supplied by natural gas, distillate oil, residual oil, and steam, respectively:

$$e_{heat} = p_{natgas} * e_{natgas} + p_{dist} * e_{dist} + p_{resid} * e_{resid} + p_{steam} * e_{steam} \qquad [16]$$

The value of e_{heat} is 203 tons per GWh;[28] the values of all parameters in Equation [16] are shown in Table 3.

Base CO_2 emissions for node *n* are:

$$CO2_{base,n} = e_{grid} * (elcb_n + ecool_n) + e_{heat} * PE_{base,heat,n} \qquad [17]$$

Emissions associated with cogeneration at node *n* are simply:

$$CO2_{cog,n} = e_{natgas} * PE_{cog,n} \qquad [18]$$

Therefore, the *local* reduction in CO_2 emissions at node *n* is:

$$benefit_{CO_2,local,n} = CO2_{cog,n} - CO2_{base,n} \qquad [19]$$

The reduction in CO_2 emissions associated with displaced grid electricity is:

$$CO2_{displ,n} = e_{grid} * (esold_n) \qquad [20]$$

The *system* reduction in CO_2 emissions at node *n* is then:

$$benefit_{CO_2,system} = \sum_{n=1}^{N} (benefit_{CO_2,local,n} - CO2_{displ,n}) \qquad [21]$$

Note that base CO_2 emissions citywide are:

$$CO2_{base,system} = \sum_{k=1}^{K} CO2_{base,k} \qquad [22]$$

We compare $CO2_{base,system}$ with the results of New York City's GHG emissions inventory (City of New York, 2008). In 2008, total citywide simulated CO_2-equivalent (CO_2e) emissions

[28] Approximately 5% of heating demand is met with kerosene. We group kerosene with distillate oil since the emissions coefficient for kerosene is just 1% lower than the coefficient for diesel.

were 61.5 million metric tons (MMT), of which 77% – or 47.4 MMT – were associated with electricity and heat demand in buildings, of which more than 99% were CO_2 emissions (City of New York, 2008). Simulated citywide emissions in our base case ($CO2_{base,system}$) are 47.2 MMT, a difference of less than 0.5%.

4.4.3 Capacity

We estimate cogeneration capacity at each supply node based on peak hourly electricity demand (including electricity sold to the grid):

$$\hat{D}_n = \max[\overline{D}_{n,m,t}] \;\; for\ m=1,\ldots,12;\ t=1,\ldots,6 \qquad [23]$$

where $\overline{D}_{n,m,t}$ is average hourly electricity production (cog_n) during month *m* and usage period *t*. Therefore, the additional *system* capacity associated with the cogeneration supply nodes is:

$$benefit_{cap,system} = \sum_{n=1}^{N} \hat{D}_n \qquad [24]$$

Note that capacity refers to electricity generation capacity at the node; heat availability is based on the heat-to-electric ratio of the prime mover. Depending on the technology scenario and the total load size, the node may require one or several generating units; we do not consider generator configuration within the node beyond assuming that at least one generator will be located in the anchor building. We also do not account for spare capacity that may be required to maintain system reliability in case of an unexpectedly large peak. These limitations aside, $Benefit_{cap,system}$ provides an estimate of distributed cogeneration capacity that could be integrated into the urban energy system.

5 Results and discussion

We find that technical potential for cogeneration exists in all five boroughs of New York City and that cogeneration can offer large benefits, particularly in terms of CO_2 emissions reductions, if implemented in all technically feasible locations. Residential neighborhoods with multi-family buildings may be good sites for cogeneration supply nodes because they tend to have thermal energy load that is several times larger than electric load.

Distributed cogeneration with small (~ 1 MW) generators could add up to 709 MW of capacity, of which 70% is outside Manhattan. This 709 MW of cogenerated electricity and heat could reduce primary energy demand by 2.4% and CO_2 emissions by 7.9%, citywide. Multi-family housing accounts for over 96% of the floor area in the supply nodes because this building function is prevalent in New York City, meets our criteria for continuous thermal sinks, and is often located on large lots identified as anchors.

Opportunities for medium (~10 MW) generators are limited by our maximum cluster size of 10 buildings, although we identify up to 8,876 MW of capacity in a block scenario. This suggests that a district energy solution, where cogeneration complements or replaces existing in-city supply, may be promising. In this scenario, medium-sized cogeneration plants could provide electricity and heat to groups of residential blocks, with additional electricity sold to commercial blocks.

5.1 Patterns of energy demand in New York City buildings

New York City is the largest and most densely populated city in the United States, but land use varies widely across the five boroughs, and this has a strong effect on patterns of energy demand and opportunities for distributed cogeneration. The majority of the city's economic activity occurs in Manhattan's Central Business District (CBD), the largest in the United States and the focal point of a $1.1 trillion metropolitan GDP (BEA, 2008). City blocks in this part of the city generally have smaller footprints, but can have more than 10 times the demand of residential blocks in the outer boroughs (Figure 2). Note that certain large lots, as defined in PLUTO, may contain many buildings; energy demand reflects the total for all buildings on the lot. For an example, see John F. Kennedy (JFK) and La Guardia (LGA) airports, which are labeled on Figure 2.

Several factors are responsible for the difference between the energy demand profile of residential and commercial areas. Both the floor area per lot and the energy intensity are higher in commercial buildings, increasing total load on commercial lots. The fraction of total load that is base electric (lighting, appliances, etc.) is also higher (Figure 3), and the diurnal demand profile is more pronounced, with peak electricity demand typically occurring during the afternoon on weekdays (Figure 4).[29] These factors make it unlikely that commercial buildings will be continuous thermal sinks, and thus they are rarely identified as anchors in our model.[30]

On the other hand, since commercial buildings tend to produce more than enough waste heat to cover thermal demand, they can be candidates for isolated, or "islanded," systems, although not all waste heat may be used, reducing thermal efficiency and associated benefits. We did not pursue island scenarios because pilot runs with the model revealed that primary energy demand could increase substantially in such scenarios where there is no thermal sink for waste heat.[31]

[29] Coincidence between electricity and space heating demand on winter days also tends to be lower in commercial buildings since space heating demand declines as the ambient air temperature rises, and as buildings fill up with workers. Further research is needed to characterize this aspect of diurnal variation in the model.

[30] Since individual buildings can have multiple functions, some mixed-use commercial buildings can be continuous thermal sinks.

[31] This situation could change dramatically if the Con Edison steam system served as a thermal sink for buildings in Manhattan south of 96th street, similar to how the electricity grid can serve as a sink for extra electricity produced at cogeneration supply nodes. See Consumer Power Advocates (2009). Cogeneration systems that produce less waste

Residential buildings are often thermal sinks because thermal load is several times higher than electric load annually, there is substantial demand for hot water, and there is less diurnal variation in demand (see Figure 4). In multi-family buildings, 46% of annual thermal load intensity is associated with hot water (versus 24% for 1-4 family homes), which makes these buildings particularly good anchor building candidates. Multi-family buildings differ from low-density housing because they tend to house more people per floor area in smaller housing units. This increases hot water intensity, which scales with the number of people, and decreases space heating intensity, since less heat is lost through building walls. Also, in large, multi-family buildings, individual tenants have less control over their thermostats and different tenants may be home at different times, which can dampen diurnal variation in demand.

In New York City, there are about 3.5 times more HDD than CDD, but heating/cooling intensity per HDD/CDD varies by building type (Figure 5). For example, office buildings and stores require less heat to stay warm in the winter and more cooling to stay cool in the summer. Therefore, cooling intensity per CDD exceeds heating intensity per HDD in these buildings. The opposite is true in residential buildings, and the relationship varies for other types of commercial and institutional buildings, depending on their function.

heat per unit of electricity produced, such as large, combined cycle gas turbines, might be a better fit for the demand profile of office buildings. Also, an electric or hybrid chiller, rather than an absorption chiller, might increase the overall thermal efficiency of cogeneration systems in offices.

a)

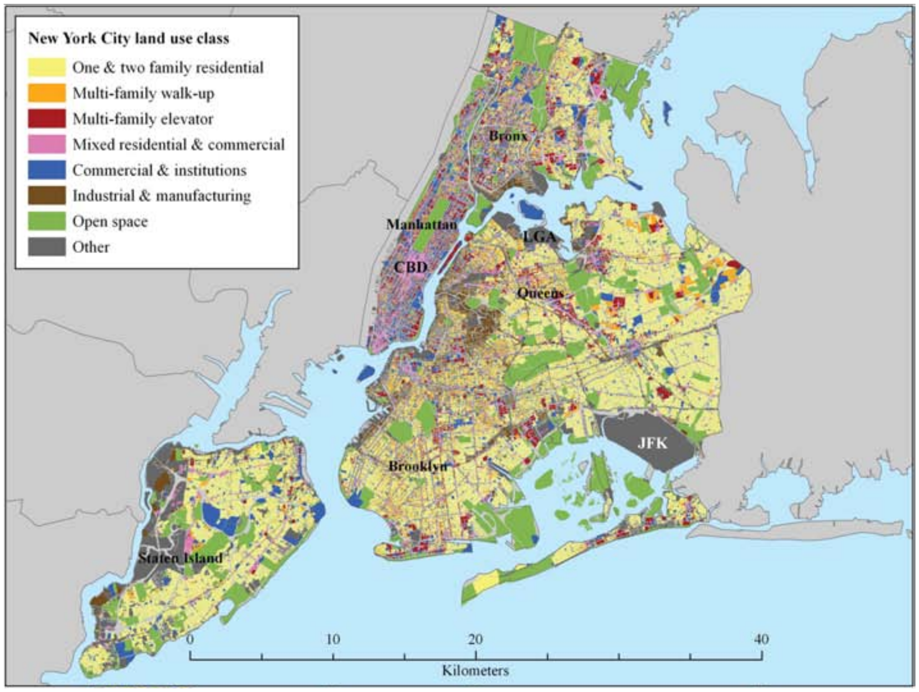

b)

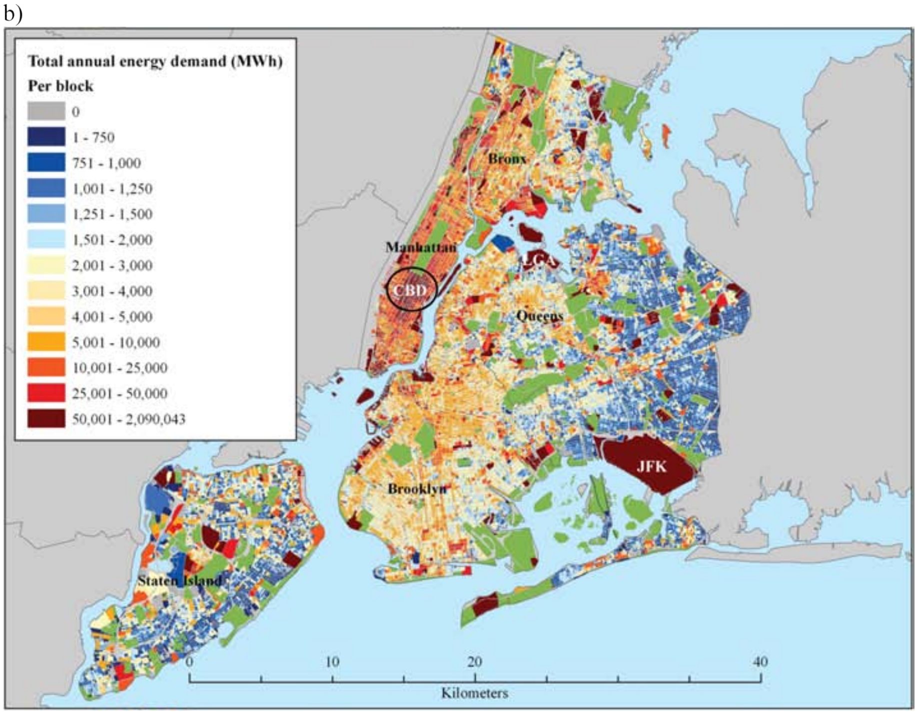

Figure 2. Patterns of land use and energy demand, measured as annual building loads. a) New York City land use classification from PLUTO. Note that multiple building functions may be present within each land use class. b) Simulated total annual demand in MWh for each New York City block. The central business district (CBD), La Guardia airport (LGA), and John F. Kennedy airport (JFK) are labeled.

DRAFT – Do not cite or quote without the permission of the authors.

a)

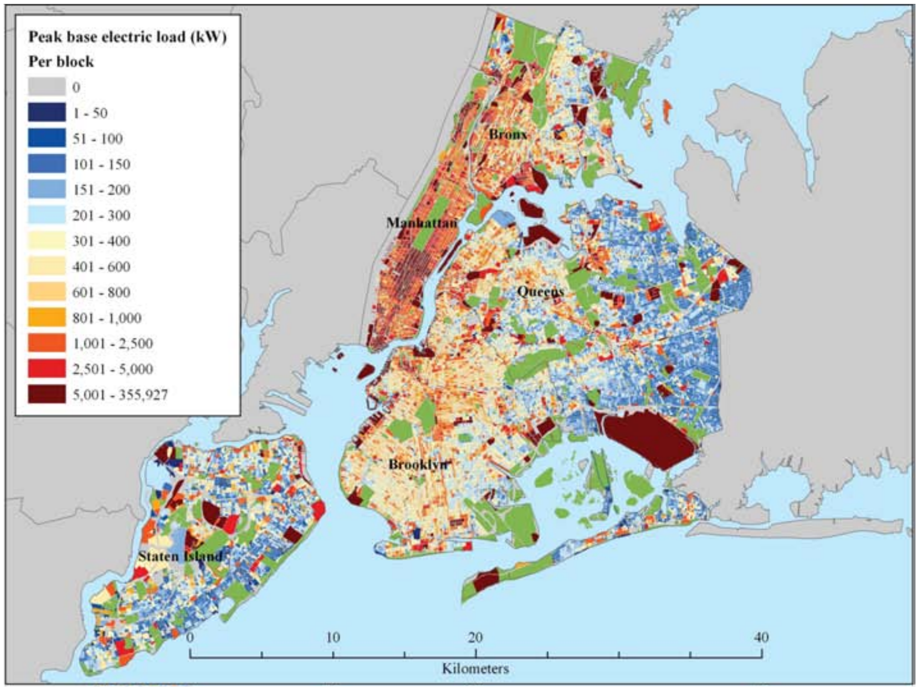

b)

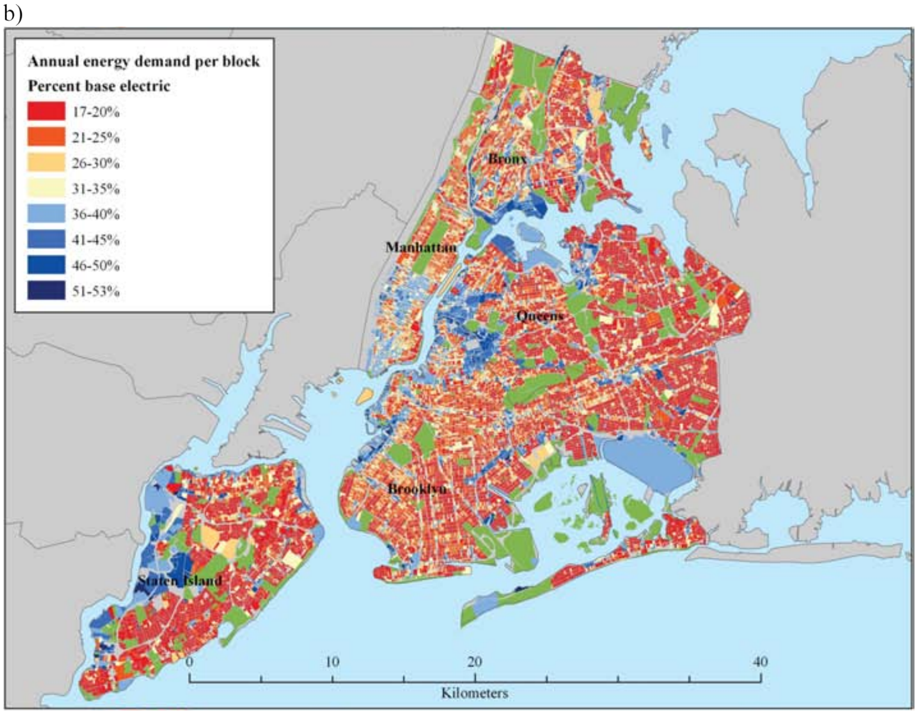

Figure 3. Patterns of electricity consumption. a) Simulated peak load in kW on each block, where peak load is the maximum hourly base electric load. b) Percent of total annual load that is base electric.

DRAFT – Do not cite or quote without the permission of the authors.

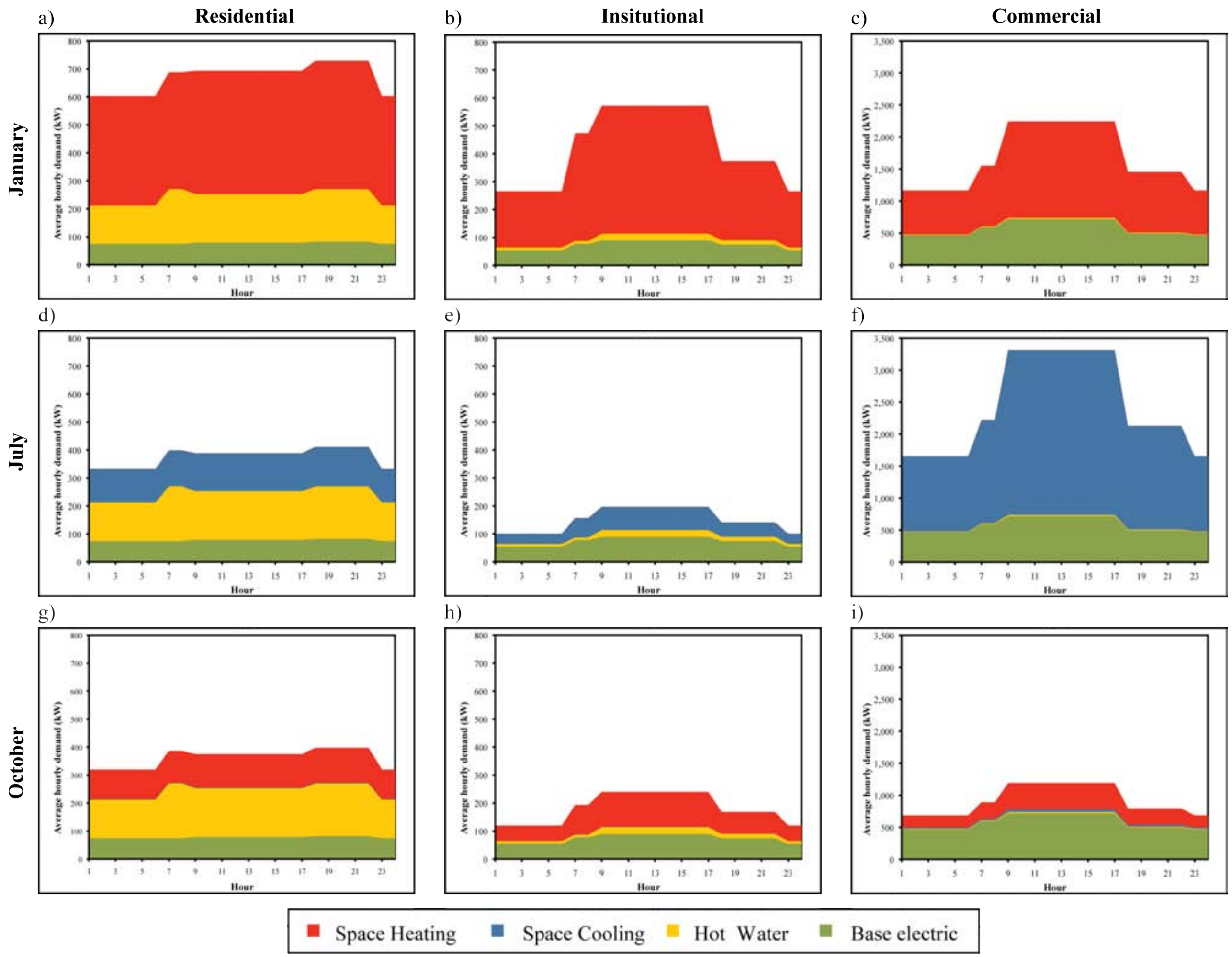

Figure 4. Simulated diurnal weekday load shapes for 3 building functions. (a) Multi-family residential, January. (b) Education, January. (c) Commercial office, January. (d) Multi-family residential, October. (e) Education, July. (f) Commercial office, July. (g) Multi-family residential, October. (h) Education, October. (i) Commercial office, October.

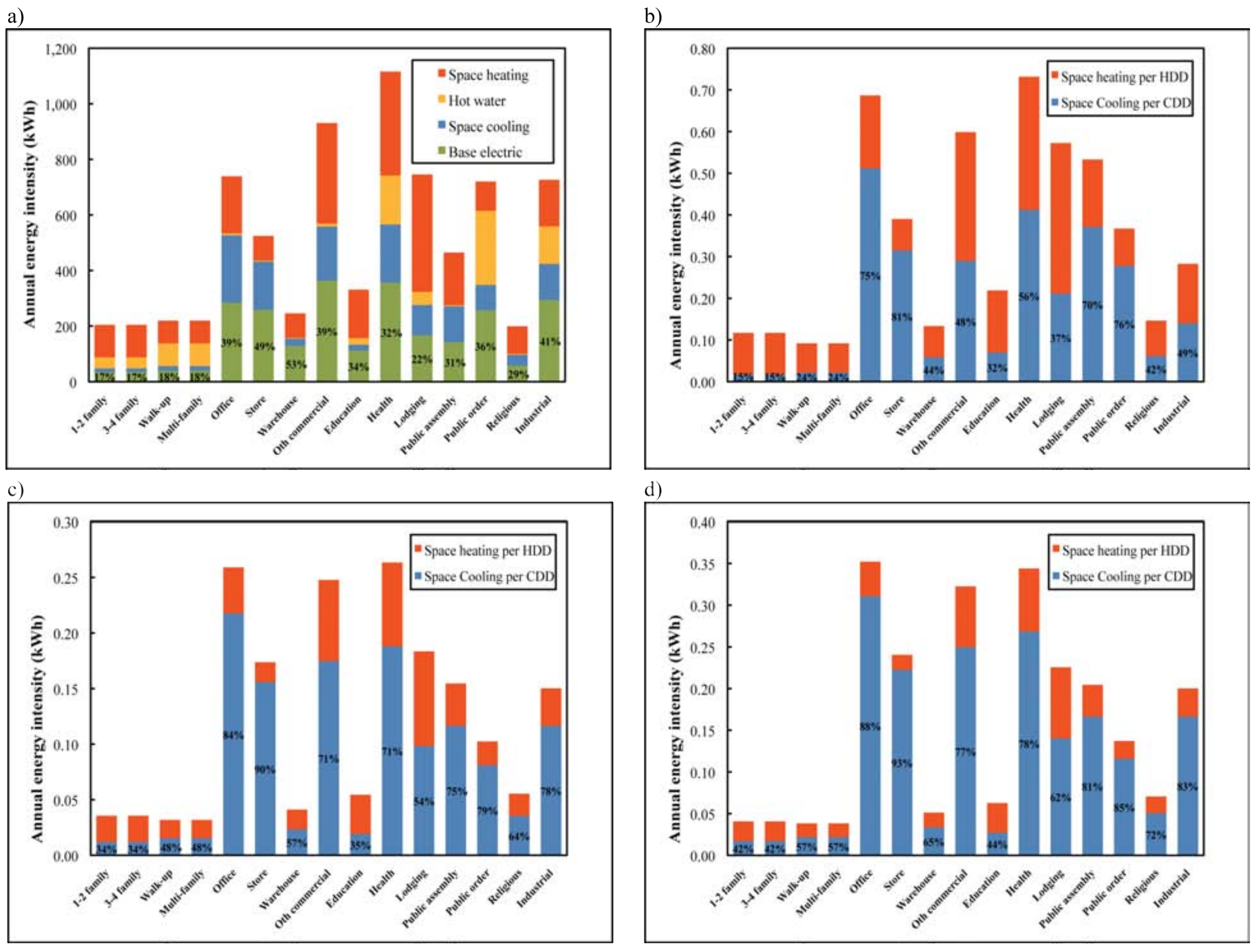

Figure 5. Annual end-use intensities for each building function. (a) Annual building load intensity. (b) Space conditioning intensity per HDD/CDD in the base case, with electric chiller and boiler. (c) Space conditioning load intensity per HDD/CDD. (d) Space conditioning intensity per HDD/CDD in the cogeneration case, with absorption chiller.

Space conditioning intensities also vary depending on the source of space heating and cooling. In most cities, electricity is the source of space cooling and direct fuel consumption is the source of heat. Electric chilling reduces the intensity of space cooling because electric chillers provide several units of cooling output for each unit of electricity input. Absorption chillers have the opposite effect since a single-effect absorption chiller produces less than one unit of cooling output for each unit of heat input. In commercial buildings, which are cooling-dominant in New York, the difference between CDD intensity and HDD intensity increases if an absorption chiller is used. In residential buildings, which are heating-dominant, an absorption chiller helps to balance these intensities, provided that the building has air conditioning. This is another reason why we find that our technology scenarios, which include an absorption chiller, are a better match for multi-family buildings.[32]

Our evaluation of the technical potential, rather than the economic viability of cogeneration, as well as the inclusion of an absorption chiller and our condition that cogeneration supply nodes must be *continuous* thermal sinks, helps explain why we find that multi-family buildings represent a large opportunity for cogeneration in the city. This finding contrasts NYSERDA (2002), which identified institutional and commercial buildings as sectors of opportunity on the basis of their annual thermal-to-electric ratio, total load size, and market potential in these sectors. Similar to King (2006), we also show that load profile, not annual ratios, determines cogeneration feasibility. For example, the load profile of many commercial buildings implies they are good candidates for peak-shaving strategies, or for operational optimization – i.e., where the system is operated only at times when it is cheaper to cogenerate

[32] Note that our estimates of annual cooling intensity are citywide averages for each building function, so they are influenced by air conditioning penetration, which is approximately 84% in residential buildings, after accounting for both window AC (67% of units) and central AC (17% units) (US Census, 2004). Therefore, cooling intensity may be underestimated for buildings with AC and overestimated for buildings without AC.

electricity than to purchase it. Also, in our analysis, total load size on an individual lot is less important because we assume that multiple lots can be clustered into a micro-grid.

Since 66% of New York City's floor area is residential, more than half of which is multi-family (including walk-ups), we find many opportunities where these buildings could become cogeneration supply nodes. Commercial and institutional buildings often become part of nodes that also include some multi-family floor area but are rarely identified as stand-alone nodes in scenarios with small gas turbines. If load size indicates that medium gas turbines make sense, commercial and institutional floor space in the nodes increases because the electric-to-heat ratio of a medium turbine is higher than with a small turbine.

5.2 Technology scenario results

Our technology scenarios were designed to explore the boundaries of the technical potential for distributed cogeneration in the city – both for restrictive scenarios requiring an anchor building with a minimum size and unrestrictive scenarios at the block scale. In our most restrictive small-turbine scenario, which requires a building footprint of 2500 m^2 and excludes the area of Manhattan served by the district steam system, we find that 575 MW of cogeneration capacity could reduce primary energy demand by 1.8% and CO_2 emissions by 6.2% (Table 4). This is approximately 28% lower than the PlaNYC goal of 800 MW.

Table 4. Cogeneration technology scenario results.

Scale:	Buildings			Blocks		
Scenario:	**1**	**2**	**3 (d)**	**4**	**5**	**6 (e)**
Gas turbine size (small~1MW, medium~10 MW): (a)	**small**	**small**	**medium**	**small**	**small**	**medium**
Absorption chiller (single-effect with COP=0.7):	**yes**	**yes**	**yes**	**yes**	**yes**	**yes**
Anchor definition (f=footprint, g=gross floor area): (b)	**>2.5K f**	**>2.5K f**	**>2.5K f**	**>32.5 g**	**none**	**none**
Steam system territory included? (c)	**yes**	**no**	**yes**	**yes**	**yes**	**yes**
Additional capacity (based on max load) (MW)	**709**	**575**	**140**	**660**	**2,467**	**8,876**
Manhattan (MW) [% of additional capacity]	214 [30%]	81 [14%]	78 [45%]	311 [47%]	782 [32%]	2102 [24%]
Bronx (MW) [% of additional capacity]	165 [23%]	165 [29%]	77 [45%]	115 [17%]	470 [19%]	1365 [15%]
Brooklyn (MW) [% of additional capacity]	166 [23%]	166 [29%]	0 [0%]	130 [20%]	681 [28%]	2570 [29%]
Queens (MW) [% of additional capacity]	150 [21%]	150 [26%]	16 [10%]	96 15%]	484 [20%]	2220 [25%]
Staten Island (MW) [% of additional capacity]	13 [2%]	13 [2%]	0 [0%]	9 [1%]	50 [2%]	618 [7%]
Base annual primary energy demand within supply nodes (GWh)	12,852	9,990	1,435	10,723	38,626	91,974
Change in primary energy demand within supply nodes (%)	+28.1%	+33.5%	+104.6%	+44.2%	+46.0%	+55.9%
Change in primary energy demand system-wide (%)	**-2.4%**	**-1.8%**	**-0.2%**	**-1.7%**	**-5.2%**	**-18.2%**
Base annual CO_2 emissions within supply nodes (MMT)	2.77	2.15	0.3	2.31	8.4	20.0
Change in CO_2 emissions within supply nodes (%)	+7.6%	+12.2%	+70.7%	+21.1%	+22.3%	+29.9%
Change in CO_2 emissions system-wide (%)	**-7.9%**	**-6.2%**	**-1.3%**	**-6.8%**	**-23.2%**	**-72.2%**
Number of supply nodes (either building clusters or blocks)	723	639	7	562	4,117	20,418
Average building cluster size (number of tax lots per cluster)	1.43	1.38	1.43	1.10	-	-
Tax lots included in supply nodes (% of New York City total)	**0.12%**	**0.10%**	**<0.01%**	**0.07%**	**12.7%**	**79.1%**
Total floor area within supply nodes (million m^2)	38	31	4	36	132	300
Floor area within supply nodes (% of New York City total)	**8.0%**	**6.5%**	**0.84%**	**7.6%**	**27.7%**	**63.0%**
1 & 2 family (% of total floor area)	0.0%	0.0%	0.0%	0.0%	8.7%	31.3%
3 & 4 family (% of total floor area)	0.0%	0.0%	0.0%	0.0%	4.4%	7.8%
Walk-up (% of total floor area)	1.1%	1.3%	0.0%	0.2%	18.0%	13.4%
Multi-family (% of total floor area)	**96.2%**	**96.3%**	**89.8%**	**97.9%**	**64.6%**	**39.0%**
Education (% of total floor area)	0.9%	0.9%	0.0%	0.0%	0.5%	1.2%
Health (% of total floor area)	0.0%	0.0%	0.0%	0.0%	0.1%	0.6%
Lodging (% of total floor area)	0.1%	0.1%	7.4%	0.1%	0.3%	0.8%
Public Assembly (% of total floor area)	0.0%	0.1%	0.0%	0.1%	0.2%	0.3%
Public Order (% of total floor area)	0.0%	0.0%	0.0%	0.0%	0.0%	0.0%
Religious (% of total floor area)	0.2%	0.2%	0.0%	0.0%	0.6%	1.1%
Office (% of total floor area)	0.3%	0.2%	0.4%	0.3%	0.5%	0.9%
Store (% of total floor area)	0.9%	0.7%	2.3%	1.0%	1.8%	2.6%
Warehouse (% of total floor area)	0.0%	0.0%	0.0%	0.0%	0.1%	0.3%
Other Commercial (% of total floor area)	0.2%	0.2%	0.2%	0.4%	0.2%	0.5%
Industrial (% of total floor area)	0.1%	0.1%	0.0%	0.0%	0.0%	0.2%

(a) Additional parameters for each prime mover, including thermal efficiencies, are shown in Appendix Table 2. (b) In all scenarios, we exclude 1-4 family residential lots and lots designated as parks from the set of possible anchor buildings. (c) In the scenario where the steam system is excluded, buildings between the southern tip of Manhattan and 96th street are excluded. This approximates the service territory of the Con Edison district steam system. (d) In this scenario, only individual building clusters with at least 10 MW of capacity are retained, where capacity is estimated from peak electric demand. (e) In this scenario, all blocks that match the heat-to-electric ratio of a medium turbine are identified, regardless of the block's load size. We assume that groups of co-located blocks could be clustered into cogeneration supply nodes with 10 MW+ base electric demand.

Currently, the steam system primarily serves commercial and industrial customers, whereas our scenarios primarily identify residential buildings as supply nodes. When the steam system zone is included, we find that 709 MW of capacity (~11% lower than the PlaNYC goal) could reduce energy demand by 2.4% and CO_2 emissions by 7.9%. Reducing the size threshold for an anchor building and/or allowing for other types of prime movers could increase potential capacity and system benefits. Figure 6 shows the spatial distribution of supply nodes in this scenario, with 30% of cogeneration capacity located in Manhattan. In the scenario where anchor buildings must have 32,515 m^2 of gross floor area, aggregate capacity is smaller (660 MW), but 47% of this is in Manhattan. New York City land use patterns are a key factor: 60% of the lots with floor area above 32,515 m^2, but just 7% of lots with footprints above 2500 m^2, are located in Manhattan.

In the small-turbine scenarios, we assume that no load is too small to be supplied by a small gas turbine. But in the scenario that has an aggregate capacity of 709 MW, loads range from 45 kW to 22.5 MW, with a median load size of 606 kW and a mean of 981 kW. Nodes with a capacity less than 500 kW account for about 14% of the total capacity in this scenario, and nodes with a capacity between 500 kW and 1 MW account for another 20% of capacity. In practice, very small nodes probably are best served by microturbines or another alternative prime mover, and very large nodes probably are best served by a small number of medium turbines rather than a large number of small turbines.

Since the heat-to-electric ratio of medium turbines is significantly higher than the ratio for small turbines, a larger number of buildings have a matching demand profile. But, medium turbines cannot be deployed in small nodes. Therefore, we identify only 7 nodes with an aggregate capacity of 140 MW. In this scenario, a larger share of floor area is non-residential: 7.4% is lodging and 2.3% is stores.

Our block-scale scenario with medium turbines is intended to converge on a citywide district energy solution. In this scenario, we remove the constraint that individual nodes must have at least 10 MW of demand since, in a district energy system, the intention is to create a large network with a smaller ratio of generators to demand nodes. We find potential capacity of 8,876 MW, more than 8 times the existing cogeneration capacity and larger than current electricity generation capacity in New York City. About 70% of city blocks are covered in this scenario (Figure 8). Results indicate a 72.2% reduction in CO_2 emissions, 9 times larger than any of the building scenarios, but not inconsistent with the larger total capacity of the scenario.

Results also reveal that generators should be located in residential neighborhoods, where demand for thermal energy is highest, with extra electricity available for commercial areas. Many of the blocks identified include low-density housing, which we assume has relatively high thermal demand throughout the day, as well as coincident electric and thermal demand. In reality, occupants of single-family homes tend to exert more control over space conditioning needs, so thermal demand may be more variable than in multi-family housing.

A common feature of all the scenario results is local increases, but system decreases, in primary energy demand and CO_2 emissions. This occurs because supply nodes must generate more electricity than is required to meet their base electric demand. Also, in all the scenarios, the system-wide CO_2 emissions reduction is at least several times larger than the system-wide reduction in primary energy demand. Although cogeneration supply nodes displace a larger amount of heat than electricity, the CO_2 emission reduction per unit of displaced electricity is larger. Therefore, as the amount of electricity sold increases, the CO_2 emissions reduction per unit reduction in primary energy demand increases. The shift from electric chilling to absorption chilling further amplifies this effect by increasing cogeneration system size and thus the amount of electricity sold. Note that if the supply node has a thermal-to-electric ratio such that very little electricity is sold, then percent reductions in primary energy demand and CO_2 emissions are very similar. These findings highlight the importance of fully integrating cogeneration supply nodes into the urban energy system to achieve maximum benefits.

The limited set of technology scenarios presented in this paper have illustrated some of the possible benefits of pursuing distributed cogeneration in New York City, but further research is needed to obtain more robust estimates of potential energy and emissions reductions and cogeneration capacity. Evaluation of additional scenarios – such as scenarios without an absorption chiller or that do not require a large anchor building – as well as refinement of building load and technology parameters – could improve estimates of the potential benefits of cogeneration.

Estimates could also be improved through the explicit incorporation of uncertainty in model parameters. In each technology scenario, the model was run a single time with a set of parameters representing best-guess average values for building loads and technologies. Estimating average building loads in New York City was difficult due to lack of data, and particularly data disaggregated by end use or time of day. Further, average values obscure variability in load intensity within each building function that could be better represented with probability distributions. Average values also do not account for variation in heating and cooling loads due to climate variability and change.

Errors in the model's building load profiles are likely to be the largest source of error because they determine the computed thermal-to-electric ratios, and can thus alter which nodes are identified in the cogeneration technology scenarios. Errors in technology characterization can have the same effect, but technology data is of higher quality than building data, and variation in performance is smaller than variation in building loads. Still, even small errors in technology characterization could shift some types of buildings above or below the threshold for a cogeneration match, dramatically altering model results.

Analysis of the sensitivity of results to uncertainty in parameter values could help to identify the magnitude of possible errors and establish the upper and lower boundaries of cogeneration potential. This could be accomplished through the use of Monte Carlo simulation and probability distributions for key input parameters, similar to the method described in Weber et al. (2009). In Monte Carlo simulation, the most likely range of output values is estimated by running a series of simulations with different input values, where the input values are generated from probability distributions. In cases where there is substantial uncertainty in input data, this technique is an improvement over uncertainty analysis based on a small number of discrete scenarios.

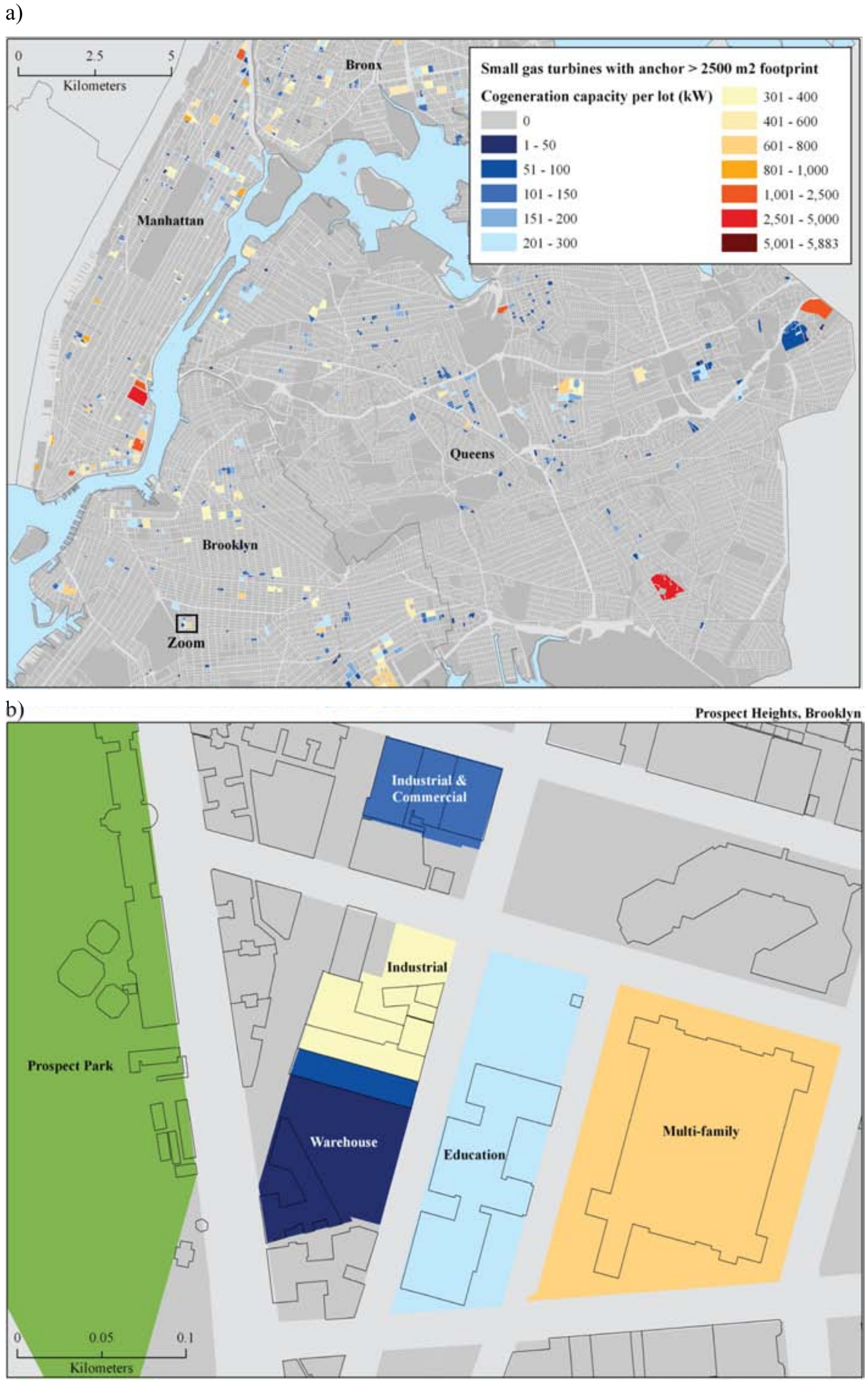

Figure 6. Results of building-scale cogeneration with small gas turbines and anchor buildings with footprint of at least 2500 m^2. a) Spatial distribution and capacity of cogeneration supply nodes in part of New York City. b) Zoom of lots identified in Prospect Heights, Brooklyn.

a)

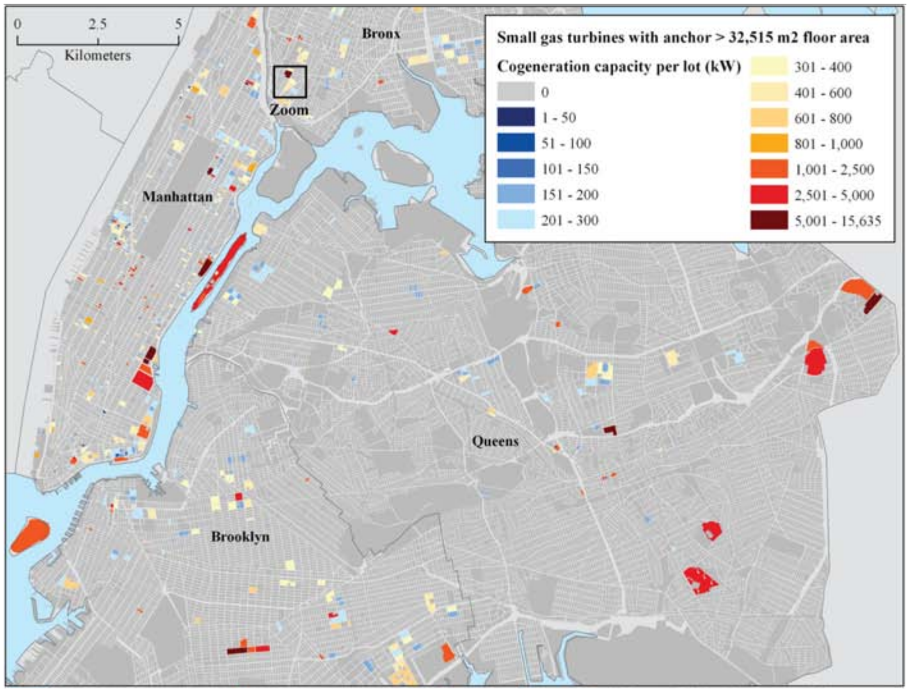

b) South Bronx

Figure 7. Results of building-scale cogeneration scenario with small gas turbines and anchor buildings with gross floor area of at least 32,515 m^2. a) Spatial distribution and capacity of cogeneration supply nodes in part of New York City. b) Zoom of lots identified in the South Bronx.

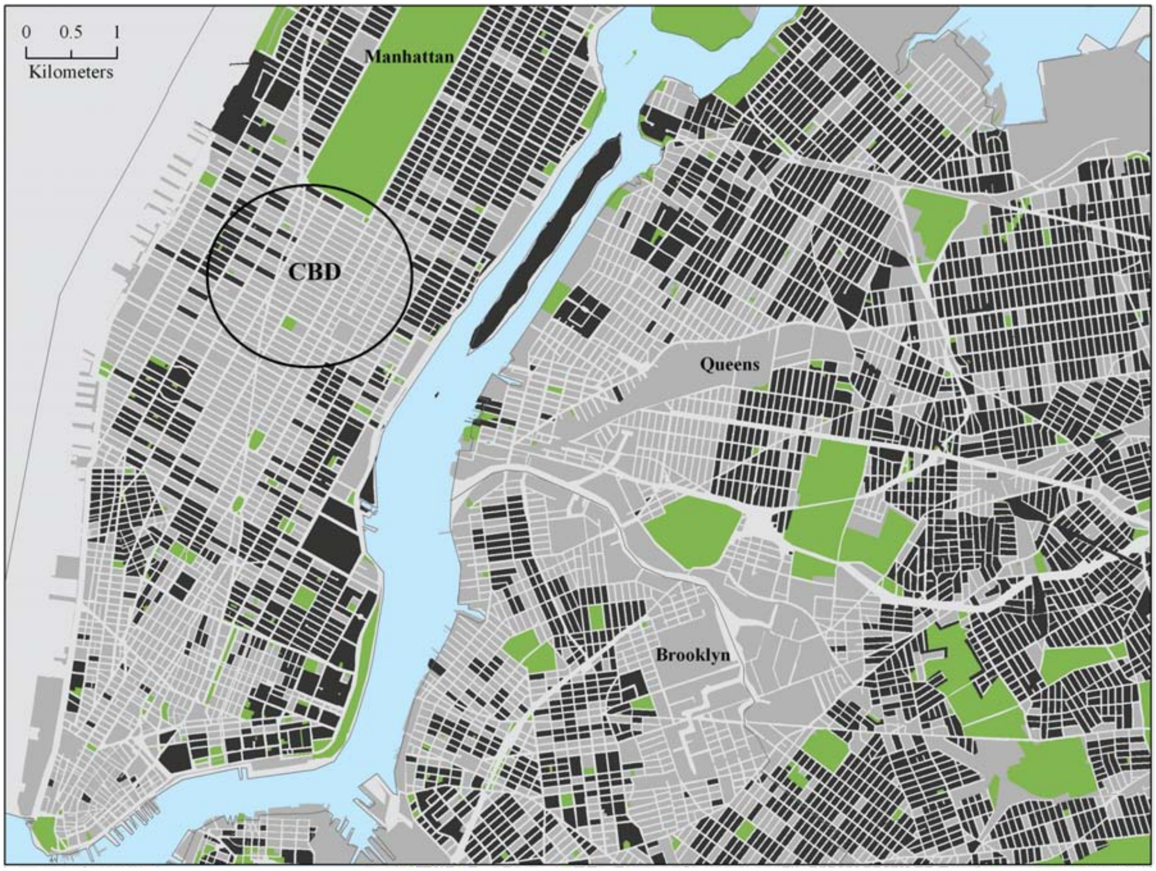

Figure 8. Blocks identified in cogeneration scenario with medium gas turbines.

6 Conclusion

We have shown how a new approach to local energy planning, in which supply nodes emerge from the fabric of demand, can contribute to alternative energy development in cities. This approach is applicable to building-scale supply options under discussion in many cities, including geothermal heat pumps, solar thermal and photovoltaic (PV) systems, and plug-in hybrids drawing electricity from city buildings. Situating supply nodes within the spatial context of urban land use can also allow for more complete analysis of the trade-offs between location-specific supply options and reductions in end-use intensities.

Distributed cogeneration may be able to deliver large reductions in CO_2 emissions if implemented in all technically feasible locations, but a complete evaluation of cogeneration potential requires analysis of the economic costs, including externalities associated with localized environmental impacts such as air pollution and noise, and uncertainties in fuel prices. An economic analysis is needed before the technology can be endorsed as a feasible strategy in any particular location. A complete evaluation would also consider the availability of gas supply and local transmission and distribution constraints, which could be incorporated into the analysis as part of further research.

Cogeneration systems can have large capital costs. The installed cost of individual generators and absorption chillers is just one component of capital cost. The price tag on multi-building cogeneration systems can climb steeply after accounting for the construction of underground pipelines to distribute heating and cooling, made more expensive by New York's density, high labor costs, and permitting requirements. Project budgets must also account for the costs of interconnection, including personnel hours to negotiate with regulators and distribution utilities. Operating costs are affected by fluctuating fuel prices, the spark spread (the difference in price between fuel and electricity), as well the applicable base tariffs (e.g. residential versus commercial, time of day pricing), and generator tariffs (e.g. standby, feed-in). Currently, New York City utilities are hesitant to embrace interconnected distributed cogeneration because of technical challenges and potential for profit loss. DG can only be a successful emissions reduction strategy if planners and regulators are able to create the right economic incentives for distribution utilities as well as local generators.

Estimation of the social cost of cogeneration requires more than just valuation of capital and operating costs since emissions of global pollutants such as CO_2, as well as local pollutants such as NO_X and SO_2, have a negative value to society. Pursuing cogeneration is a strategic decision that assumes long-term benefits, including cost savings to society, based on expectations of how the local energy system is likely to evolve. For example, the CO_2 benefits of gas-fired cogeneration may decrease if renewables become a larger share of centralized electricity supply, which is expected under mandated increases in renewable portfolio standards that are part of the current New York State Energy Plan. But, distributed cogeneration offers an alternative to large investments in new transmission capacity that may be needed to keep pace with demand growth and prevent capacity shortages during times of summer peak demand. Further research is needed to analyze the long-term benefits of distributed cogeneration under a range of future technology and policy scenarios.

One of our key findings is that maximum CO_2 reductions are achieved when electricity is sold back to the grid, but under the current tariff structure, generators rarely profit by selling electricity. Without this incentive, siting, sizing, and operation of cogeneration supply nodes is unlikely to take full advantage of New York City demand patterns. Our finding that residential neighborhoods may be good hosts for cogeneration presents siting and coordination challenges since many individual housing units must be joined into a supply node and these neighborhoods are most resistant to change. Special cases, such as large, multi-family properties owned by the New York City Housing Authority, may be good sites for early adoption.

Our model shows where there may be opportunities to locate cogeneration supply nodes that could contribute to New York City's goal of 800 MW of additional distributed generation. But the model also shows that a district energy solution may offer larger benefits than building-scale supply nodes. Detailed utility data on energy demand are needed to further evaluate the potential benefits and challenges of these scenarios.

New York City has now completed several consecutive annual GHG emissions inventories, which show that a reduction in the carbon-intensity of electricity supply is the leading factor behind a 9.0% reduction in citywide emissions of CO_2e between 2005 and 2008 (City of New York, 2009). New, more efficient electricity generation and an increase in the importation of cleaner power together were associated with a 6.5% reduction in emissions (City of New York, 2009). This confirms the importance of shifts in the fuel mix as a key strategy for achieving a 30% reduction in CO_2 emissions by 2030. But it also highlights the challenges of this ambitious goal: Based on our scenarios, approximately 2500-3500 MW of distributed cogeneration would need to come online within the next 20 years to achieve a 30% reduction in building-sector emissions; 3500-4500 MW would be needed to achieve a 30% reduction in citywide emissions. This represents 40-50% of current electricity generation capacity sited within New York City.

Many cities have set local energy efficiency and climate change mitigation targets Meeting these targets will require layering multiple technology and policy strategies into the built environment. The analytical approach we develop in this paper allows different options to emerge from urban patterns of demand and can help cities identify the most promising directions for local energy planning.

7 References

Abu-Sharkh, S., Arnold, R.J., Kohler, J., Li, R., Markvart, T., Ross, J.N., Steemers, K., Wilson, P., and Yao, R., 2006. Can microgrids make a major contribution to UK energy supply? *Renewable and Sustainable Energy Reviews*, 10, 78-127.

Andrews, C.J., 2008. Energy conversion goes local: Implications for planners. *Journal of the American Planning Association*, 74 (2), 231-254.

Center for Energy, Marine Transportation and Public Policy (CEMTPP), 2007.*CHP in NYC: A Viability Assessment*. Available at: http://energy.sipa.columbia.edu/Research/urbanenergy1.html, accessed October 2009.

Chen, H., Ooka, R., Iwamura, K., Huang, H., Yoshizawa, N., Miisho, K., Yoshida, S, Namatame, S., Sakakura, A., and Tanaka, S., 2008. Study on sustainable redevelopment of a densely built-up area in Tokyo by introducing a distributed local energy supply system. *Energy and Buildings*, 40, 782-792.

City of New York, 2004.*New York City Energy Policy: An Electricity Resource Roadmap*. New York City Energy Policy Task Force.

_________________, 2007a. *PlaNYC: A Greener, Greater New York. Mayor's Office of Long Term Planning and Sustainability*. Available at: http://www.nyc.gov/html/planyc2030/html/downloads/download.shtml, accessed July 2009.

_________________, 2007b. Personal communication with Jonathan Dickinson, Senior Policy Advisor, New York City Office of Operations, Office of Long Term Planning and Sustainability.

_________________, 2008. Inventory of New York City Greenhouse Gas Emissions, September 17, 2008; updated February 24, 2009. Available at: http://www.nyc.gov/html/planyc2030/html/emissions/emissions.shtml, accessed July 2009.

_________________, 2009. Inventory of New York City Greenhouse Gas Emissions, September 2009.

Crawley, D.B., Hand, J.W., Kummert, M., Griffith, B.T., 2005. Contrasting the capabilities of building energy performance simulation programs. In *Proceedings of Building Simulation 2005*, 15-18 August 2005, Montreal, Quebec, Canada. IBPSA.

Dhakal, S. and Hanaki, K., 2002. Improvement of urban thermal environment by managing heat discharge sources and surface modification in Tokyo. *Energy and Buildings*, 34 (1), 13-23.

Consumer Power Advocates, 2009. Proposal for Customer Sited Supply of Consumer Power Advocates. Submitted to State of New York Public Service Commission, Case 09-S-0029.

Energy Blueprint, 2009. Fossil fuel technologies. Available at: http://www.energyblueprint.info/24.0.html, accessed August 2009.

Gulli, F., 2006. Social choice, uncertainty about external costs and trade-off between intergenerational environmental impacts: The emblematic case of gas-based energy supply decentralization. *Ecological Economics*, 57, 282-305.

Gurney, K.R., Seib, B., Ansley, W., Mendoza, D., Miller, C., Fischer, M., 2008. Vulcan Science Methods Documentation. Project Vulcan, Purdue University.

Gustafsson, S-I. and Ronnqvist, M., 2008. Optimal heating of large block of flats. *Energy and Buildings*, 40, 1699-1708.

Heiple, S. and Sailor, D., 2008. Using building energy simulation and geospatial modeling techniques to determine high resolution building sector energy consumption profiles. *Energy and Buildings*, 40, 1426-1436.

Huang, J., Akbari, H., Rainer, L., and Ritschard, R., 1991. *481 Prototypical Commercial Buildings for 20 Urban Markets*. Lawrence Berkeley Laboratory for Gas Research Institute. GRI-90/2036 and LBL-29798.

International Energy Agency (IEA), 2008. *World Energy Outlook 2008*. OECD/IEA. 578 pages.

Jaccard, M., Failing, L., and Berry, T., 1997. From equipment to infrastructure: Community energy management and greenhouse gas emission reduction. *Energy Policy*, 25 (13), 1065-1074.

Jayamaha, L., 2006. *Energy-Efficient Building Systems: Green Strategies for Operation and Maintenance*. McGraw-Hill Professional, 288 pages.

King, D., 2006. *Electric power micro-grids: Opportunities and challenges for an emerging distributed energy architecture*. Doctoral dissertation, Carnegie Mellon University.

Krause, F., Koomey, J., Becht, H., Olivier, D., Onufrio, G., and Radanne, P., 1994. Energy Policy in the Greenhouse. Volume Two, Part 3C. Electricity Sourcebook. The Cost of Fossil Power Generation in Western Europe. International Project for Sustainable Energy Paths (IPSEP).

National Renewable Energy Laboratory (NREL), 2008. National Solar Radiation Data Base, 1991-2005 Update: Typical Meteorological Year 3. Available at: http://rredc.nrel.gov/solar/old_data/nsrdb/1991-2005/tmy3/, accessed August 2009.

New Buildings Institute, 1998. Absorption Chillers Guideline. Available at: http://www.newbuildings.org/guidelines.htm, accessed September 2009.

New York City Department of City Planning (NYC Planning), 2008. MapPLUTO (Release 07C) New York: NYC Department of City Planning.

New York State Energy Research and Development Authority (NYSERDA), 2002. *CHP Market Potential for New York State (Final Report 02-12)*.

Oak Ridge National Laboratory, 2006. ORNL CHP Capacity Optimizer. Available at: http://apps1.eere.energy.gov/buildings/tools_directory/software.cfm/ID=495/pagename=alpha_list, accessed July 2009.

__________________________, 2009. BCHP Screening Tool. Available at: http://www.coolingheatingpower.org/about/bchp-screening-tool.php, accessed July 2009.

Sadownik, B. and Jaccard, M., 2001. Sustainable energy and urban form in China: The relevance of community energy management. *Energy Policy*, 29, 55-65.

Thumann, A. and Mehta, D.P., 2008. *Handbook of energy engineering, 6th ed.* Liburn, GA: Fairmont Press, 460 pages.

United States Department of Commerce, Bureau of Economic Analysis (US BEA), 2008. Regional Economic Accounts. Available at: http://www.bea.gov/regional, accessed November 2008.

United States Department of Commerce, Census Bureau (US Census), 2004. *American Housing Survey for the New York-Nassau-Suffolk-Orange Metropolitan Area: 2003*.

United States Department of Energy (US DOE), Energy Information Administration, 2003. Commercial Building Energy Consumption Survey. Available at: http://www.eia.doe.gov/emeu/cbecs/, accessed July 2009.

Weber, C.L., Koomey, J.G., and Matthews, H.S., 2009. The energy and climate change impacts of different music delivery methods. Final report to Microsoft Corporation and Intel Corporation.

Yamaguchi, Y., Shimoda, Y., and Mizuno, M., 2007. Proposal of a modeling approach considering urban form for evaluation of city level energy management. *Energy and Buildings*, 39 (5), 580-592.

United States Environmental Protection Agency (US EPA), 2002. eGRID 2002 Archive. Available at: http://www.epa.gov/cleanenergy/energy-resources/egrid/archive.html, accessed September 2008.

__________________________, 2009. Catalog of CHP Technologies. Available at: http://www.epa.gov/chp/basic/catalog.html, accessed July 2009.

Table A1. Percent above or below average hourly demand in each usage period for each building function. The usage periods representing peak demand for each building function are in bold.

Building function	Base electric (%)						Space cooling (%)					
	Wkdy 6-8	Wkdy 8-5	Wkdy 5-10	Night 10-6	Wknd 6-12	Wknd 12-10	Wkdy 6-8	Wkdy 8-5	Wkdy 5-10	Night 10-6	Wknd 6-12	Wknd 12-10
Residential												
1 & 2 family	4%	-1%	**6%**	-4%	3%	2%	4%	2%	**9%**	-9%	7%	4%
3 & 4 family	4%	-1%	**6%**	-4%	3%	2%	4%	2%	**9%**	-9%	7%	4%
Walk-up	4%	-1%	**6%**	-4%	3%	2%	4%	2%	**9%**	-9%	7%	4%
Multi-family	4%	-1%	**6%**	-4%	3%	2%	4%	2%	**9%**	-9%	7%	4%
Institutional												
Education	22%	**41%**	12%	-17%	-9%	-15%	42%	**72%**	3%	-25%	-18%	-24%
Health	0%	**12%**	-1%	-13%	8%	6%	10%	**18%**	-1%	-10%	-1%	-1%
Lodging	8%	-4%	**24%**	-7%	-1%	3%	0%	-13%	4%	**11%**	-1%	-7%
Public Assembly (a)	28%	**43%**	-12%	-12%	-12%	-12%	29%	**82%**	-14%	-25%	-13%	-25%
Public Order	**9%**	**9%**	2%	-14%	**9%**	6%	-5%	1%	0%	**3%**	-8%	1%
Religious (a)	28%	**43%**	-12%	-12%	-12%	-12%	29%	**82%**	-14%	-25%	-13%	-25%
Commercial												
Office	28%	**43%**	-12%	-12%	-12%	-12%	29%	**82%**	-14%	-25%	-13%	-25%
Store	-11%	**16%**	6%	-11%	-2%	3%	-25%	31%	**32%**	-25%	-14%	10%
Warehouse (a)	28%	**43%**	-12%	-12%	-12%	-12%	29%	**82%**	-14%	-25%	-13%	-25%
Other Commercial (a)	28%	**43%**	-12%	-12%	-12%	-12%	29%	**82%**	-14%	-25%	-13%	-25%
Industrial	28%	**43%**	-12%	-12%	-12%	-12%	29%	**82%**	-14%	-25%	-13%	-25%

(a) Time of use data were unavailable for these buildings; therefore, time of use percentages for office buildings were assigned to these building functions.

Table A1 (continued). Percent above or below average hourly demand in each usage period for each building function. The usage periods representing peak demand for each building function are in bold.

Building function	Hot water (%)						Space heating (%)					
	Wkdy 6-8	**Wkdy 8-5**	**Wkdy 5-10**	**Night 10-6**	**Wknd 6-12**	**Wknd 12-10**	**Wkdy 6-8**	**Wkdy 8-5**	**Wkdy 5-10**	**Night 10-6**	**Wknd 6-12**	**Wknd 12-10**
Residential												
1 & 2 family	**20%**	4%	12%	-16%	5%	9%	4%	2%	**9%**	-9%	7%	4%
3 & 4 family	**20%**	4%	12%	-16%	5%	9%	4%	2%	**9%**	-9%	7%	4%
Walk-up	**20%**	4%	12%	-16%	5%	9%	4%	2%	**9%**	-9%	7%	4%
Multi-family	**20%**	4%	12%	-16%	5%	9%	4%	2%	**9%**	-9%	7%	4%
Institutional												
Education	-21%	**82%**	20%	-25%	-25%	-25%	42%	**72%**	3%	-25%	-18%	-24%
Health	**17%**	7%	-2%	-11%	11%	2%	10%	**18%**	-1%	-10%	-1%	-1%
Lodging	**10%**	2%	9%	-9%	8%	2%	0%	-13%	4%	**11%**	-1%	-7%
Public Assembly [(a)]	29%	**82%**	-14%	-25%	-13%	-25%	29%	**82%**	-14%	-25%	-13%	-25%
Public Order	9%	**44%**	-2%	-25%	5%	-3%	-5%	1%	0%	**3%**	-8%	1%
Religious [(a)]	29%	**82%**	-14%	-25%	-13%	-25%	29%	**82%**	-14%	-25%	-13%	-25%
Commercial												
Office	29%	**82%**	-14%	-25%	-13%	-25%	29%	**82%**	-14%	-25%	-13%	-25%
Store	-25%	31%	**32%**	-25%	-14%	10%	-25%	31%	**32%**	-25%	-14%	10%
Warehouse [(a)]	29%	**82%**	-14%	-25%	-13%	-25%	29%	**82%**	-14%	-25%	-13%	-25%
Other Commercial [(a)]	29%	**82%**	-14%	-25%	-13%	-25%	29%	**82%**	-14%	-25%	-13%	-25%
Industrial	29%	**82%**	-14%	-25%	-13%	-25%	29%	**82%**	-14%	-25%	-13%	-25%

(a) Time of use data were unavailable for these buildings; therefore, time of use percentages for office buildings were assigned to these building functions.